

We thank the referees for the time and effort they took to review this manuscript. It is clear that they understood the content of the manuscript.

The revisions needed were relatively straightforward. The exception was the piece in section 2 describing the theory. Both referees suggested that it should be put in an appendix, rather than in the main text. We decided to follow their suggestion as we agreed that this would improve the main flow of the paper. This meant however that more introductory sentences were needed in the main text to explain the main equations. Otherwise the readers would have difficulty in understanding where those equations were coming from. Also a couple of introductory sentences were needed at the beginning of the Appendix to lead the readers on their way. In addition, section numbering needed to be adjusted and all equation needed to be renumbered including in the Appendix, something which follows logically from this suggestion. None of this renumbering is described in detail in the ensuing notes as these would provide the editor with superfluous and irrelevant detail. As the theory is now in the Appendix we decided to insert a couple of small extra steps in the derivation there. These were omitted for sake of brevity in the original manuscript but they should hopefully help the reader a little more in understanding the step-by-step transition from radiation to proxy radiation and to the subsequent trend analysis.

Below you will find our notes which are ordered with reference to the individual comments by the referees.

Authors response to Anonymous Referee #1

Anonymous Referee #1

Review of the manuscript: “Impact of aerosols and clouds on decadal trends in all-sky solar radiation over the Netherland (1966-2015)” by Boers et al. The authors made a good work in analyzing 50-year hourly dataset of global radiation, cloudiness and visibility over the Netherland in order to quantify the contribution of aerosols and clouds to trends in all-sky radiation. They show that all trends in fractional cloudiness, clear-sky and cloud-base radiation contribute significantly to the observed trend in all-sky radiation. I suggest to consider this paper for publication after the following issues are addressed:

Authors response: We thank the referee for the comments. Below follow the comments and our answers to them:

Specific comments: - The length of the manuscript could be reduced (especially sections where the methods are described). In this way it will be easier to read the paper and to follow the discussion.

—

Author's response: This point was also brought up by Referee #2. The authors have decided to put the Method sections 2.1, 2.2, 2.3, and 2.4 in an appendix and only write down the end result (including a description of it) of the final equations, namely Eq. (17) and Eq. (21). This is a substantial reduction in the main text which improves the flow of the manuscript.

Line 121: the authors write that all-sky radiation is a function of three components: clear-sky radiation, cloud-base radiation and fractional cloudiness. How do you think that the results could change considering also the type of clouds and not only their extent?

Author's response: Interesting point. If some cloud would have shifted from ice to liquid within those fifty years, the microphysics would have changed [but to an unknown extent] which in turn could have impacted the radiation at the surface. However, then it needs to be quantified how such changes took place and perhaps more importantly how it would have impacted the radiation. This is not a feasible subtopic within this paper. Nevertheless, we decided to put in a statement alerting the reader to this potential issue.

Long term changes in cloud type could perhaps affect cloud optical properties (liquid water versus ice water) but their influence on trends is unknown and not studied here.

Line 262: the right hand side of the equation has four components. Only three of them are discussed (lines: 264-269).

Author's response: This was a remnant of a previous version of the paper. We corrected this as there are indeed four terms. All four are described now.

At line 269, the authors write that the fourth term is not shown. Clarify this point.

Author's response: This point is directly linked to the previous one. The correction to the text was made by removing 'not shown here' in line 270.

Line 325: How are estimated the last two parameters used for model calculations? -

Author's response: They come from the analysis of the Boers et al., 2015 Environmental Research Letters paper. This is now referenced:

The asymmetry parameter and the Ångström parameter are set to 0.69 and 1.5 respectively to reflect typical aerosol values derived for the Netherlands (Boers et al., 2015).

Line 430: How does the present weather sensor work? Why does the change from human observations to automatic sensor introduce a break in cloudiness series and not in visibility series?

Author's response: A statement was put in describing the working of this instrument:

The PWS detects the forward scattering of light emitted by a Near Infrared Light Emitting Diode under an angle of 42°

We suspect that the simplicity of the PWS instrument in comparison with the ceilometer has much to do with the ease of transition from human observer to instrument. In both cases an overlap period of two years was used to assess their performance. But for the PWS a simple adjustment will probably have sufficed. However, at an early stage it was noted that the transition to ceilometer posed serious problems mostly the result of the fact that the sky coverage of an individual ceilometer observation is a couple of square meters or less, while a human observer covers at least 25 km² if not more. How to manage such a transition for selected cloud cover is much more difficult than a simple PWS adjustment.

We decided not to amplify this point further in the text, except by stating for the PWS that

No discontinuity was detected at the year 2002 indicating good adjustment procedures from Human Observer to instrument at the transition time.

Lines 568-570: How do you explain this result?

Author's response: The increased in cloud cover together with a decrease in cloud optical thickness is an interesting result. The cause is unclear and contrary to [our] intuition. We could speculate on this issue but that would detract from the main results. However it is a valid point of attention so we included:

The implication is that clouds have become (optically thinner) but at the same time more frequent, the cause of which is unclear.

Technical corrections:

Check the reference at line 77;

Author's response: Yes, corrected in the references

Line 105: It is the first time that the abbreviation ACI is used in the text so it is necessary to define it (even if it is already defined in the abstract);

Author's response: yes, was done

Line 226: Define all the parameters in equation 16;

Author's response: yes, was done, but will be part of the newly formed appendix.

Some additional references are necessary, for example at lines:

298,

Author's response: this is standard definition of optical thickness, we believe that this does not need a reference.

303,

Author's response: this is the Mean Value Theorem, which we included in the text.

315,

Author's response: this is indeed an imprecise statement. We used the average value over the Netherlands based on the ERA data. So we changed in the text:

...and a value of 1000 m was used to reflect conditions over the Netherlands.

323,

Author's response: yes, this is Boers (1994), and included in the reference list

350;

Author's response: yes, this is Twomey (1977) and a huge number of others!

Check the reference at lines 584 and 676.

Author's response: yes it is Sanchez-Lorenzo, not the other way around. We corrected.

+++++

Authors response to Anonymous Referee #2

Second review of "Impact of aerosols and clouds on decadal trends in all-sky solar radiation over the Netherlands (1966-2015)," by R. Boers, T. Brandsma, and A. P. Siebesma

General comments:

This paper shows an innovative approach to isolate the sources of dimming and brightening for the Netherlands over a 50-year period. It is of high scientific significance because the trends of dimming then brightening over the period of study are well known global phenomena, but their causes are not universally consonant. Problems in documenting dimming, especially, in the early part of the period of study are hampered by a lack of appropriate data that have been generally available during the recent brightening period. In my opinion, the authors have ably used available sources of data to create credible proxies and correct data appropriately (e.g., cloud fraction over the transition from human observers to ceilometers) to study dimming and brightening over the Netherlands and impressively determined the relative contributions of aerosols and clouds to those phenomena.

We thank the Referee for the comments. Below follow the comments and our answers to them:

The mathematics used is impressive but cumbersome and could be simplified for the reader by including only the final equations in the main text of the paper, with complete descriptions of their components and the details of the derivations placed in an appendix. That is only a suggestion. In addition, more frequent reminders to the reader of the time periods that terms discussed represent would be useful.

Authors response: This point was also brought up by Referee #1. The authors have decided to put the Method sections 2.1, 2.2, 2.3, and 2.4 in an appendix and only write down the end result (including a description of it) of the final equations, namely Eq. (17) and Eq. (21). This is a substantial reduction in the main text which improves the flow of the manuscript.

One major concern is that the primary results presented in Table 2, and summarized in the abstract, are not intuitive and require more explanation. That is, the 50-year trends in clear-sky and cloud-base radiation are both greater than the 50-year trend in all-sky radiation. Intuitively, the former two trends should add to the all-sky trend. However, when examining sub-trends during the periods of dimming and brightening separately, which can be done from the results presented in Table 2, the component trends (i.e., clear-sky and cloud-base) do sum better to the reported all-sky trends for those sub-periods, within the margins of error presented.

Authors response: For the better part of a year the first author shared with Referee #2 the notion that the clear-sky and cloud-base radiation trends should add up to the all-sky trend. This is also what is implicitly stated in many studies on this subject. So we can appreciate Referee #2's difficulty in understanding the issue at hand. It was only after the third author was able to write down the equations on the separation of clear and cloudy signals that we realized how wrong we were. Intuition is not a good guide in this matter. Perhaps the simplest way to see it is to picture the 'all-sky' as partly 'clear-sky' and partly 'cloudy-sky'. This then must mean that both should be weighted by their sky fraction, and that changing the sky fraction itself should also be of importance in determining the trend. Furthermore, included in the complexity associated with understanding this analysis are the concepts associated with the separation between 'real' data and its 'proxy' counterpart. These points of Referee #2 are quite valid in our opinion and additional statements explained the results should be of assistance in understanding all of these issues, so we included at the end of the discussion of Table 2 on the proxy analysis:

Note that both the trends in all-sky radiation and the trend in all-sky proxy radiation are given in the table. The trend in all-sky radiation is simply inferred from the data whereas the trend in all-sky proxy radiation is computed from Eq. (3). Thus, contrary to common notion the trend in measured all-sky radiation cannot be recovered from the trends in proxy data. It is only the all-sky proxy trend that can be recovered from the clear-sky proxy term and the cloud-base proxy term of Eq. (3) and in addition from the fractional cloudiness term of Eq. (3). Note furthermore that the fractional cloudiness term in Eq. (3) is a scaled version of the trend in fractional cloudiness, whereas the other two are scaled versions of the trend in clear-sky proxy radiation and cloud-base proxy radiation.

Also at the end of the appendix when the trend analysis is explained we included some statements on the counterintuitive aspects of understanding the trends:

The implications of this expression are quite important. Eq. (A22) demonstrates that the trend in all-sky radiation is not a simple summation of trends in clear-sky and cloudy-sky trends, which would perhaps be an intuitive notion when seeking to explain the observed trend in all sky radiation. Eq. (A22) demonstrates that a) the trends in clear-sky and cloud-base radiation need to be weighted by their fractional occurrence in the atmosphere, and that b) there is a third term constituting the trend in fractional cloudiness scaled by the difference in average cloud-base and clear-sky radiation. Furthermore, the additional fourth term, which is shown to be negligible in the current analysis, may not always be small when there are significant cross correlations between the perturbations.

One potential problem I see in your analysis is in your interpretation of eq. 21. As stated on lines 256-257, the over-bars in the equation represent 50-year means and the primed quantities represent yearly deviations from decadal averages. This inconsistency may lead to problems. Another potential problem I see is that the weights applied to the clear-sky term (.32) and the cloud fraction term (.68) represent the fractional periods of clear and cloudy conditions over the entire 50-year period. Since those fractions likely change through the 50-year period, I believe it would be beneficial to analyze eq. 21 over decadal periods, using decadal means, yearly deviations from decadal means, and decadal weights of fractional clear-sky and cloudy periods to compute $S'(y_k)$.

Then, the means and deviations used would be internally consistent and the fractional mean periods of clear and cloudy skies would be appropriate to the decade being analyzed.

Authors response: This was an error in the text: it should read: 'yearly deviations from an average over 5 decades of the yearly averages'. We regret the confusion caused by this error. Given Referee #2 's interpretation of the erroneous text in the original manuscript the suggestions given are quite logical. However, the two time periods given in the text (1966 – 1984) and (1984 – 2015) are not multiples of a decade which impedes the analysis suggested here (the break point of 1984 would have to be changed). We prefer to leave as is (but of course corrected the error in the text which now appears in the appendix).

Specific comments:

Abstract: As detailed in the general comments, the differences among the three trends listed needs more explanation.

Authors response: Yes, the problem with the abstract is that the aspect of real data versus proxy data were not even addressed, so this point certainly needs to be amplified: We inserted a set of statements in the abstract more fully explaining what we did, which now reads as follows:

A 50-year hourly dataset of global shortwave radiation, cloudiness and visibility over the Netherlands was used to quantify the contribution of aerosols and clouds to the trend in yearly-averaged all-sky radiation ($1.81 \pm 1.07 \text{ Wm}^{-2}/\text{decade}$). Yearly averaged clear-sky and cloud-base radiation data show large year-to-year fluctuations caused by yearly changes in the occurrence of clear and cloudy periods and cannot be used for trend analysis. Therefore, proxy clear-sky and cloud-base radiations were computed. In a proxy analysis hourly radiation data falling within a fractional cloudiness value are fitted by monotonic increasing functions of solar zenith angle and summed over all zenith angles occurring in a single year to produce an average. Stable trends can then be computed from the proxy radiation data. A functional expression is derived whereby the trend in (proxy) all-sky radiation is a linear combination of trends in fractional cloudiness, (proxy) clear-sky radiation and proxy cloud-base radiation. Trends (per decade) in fractional cloudiness, (proxy) clear-sky and (proxy) cloud-base radiation were respectively 0.0097 ± 0.0062 , $2.78 \pm 0.50 \text{ Wm}^{-2}$, and $3.43 \pm 1.17 \text{ Wm}^{-2}$. To add up to the (proxy) all-sky radiation the three trends have weight factors, namely the difference between the mean cloud-base and clear-sky radiation, the clear-sky factor (1-fractional cloudiness) and the fractional cloudiness, respectively. Our analysis clearly demonstrates that all three components contribute significantly to the observed trend in all-sky radiation. Radiative transfer calculations using the aerosol optical thickness derived from visibility observations indicate that Aerosol Radiation Interaction (ARI) is a strong candidate to explain the upward trend in the clear-sky radiation. Aerosol Cloud Interaction (ACI) may have some impact on cloud-base radiation, but it is suggested that decadal changes in cloud thickness and synoptic scale changes in cloud amount also play an important role.

l. 28-30 Brightening in the U.S. from the mid 1990s to ~2011 is attributed primarily to a reduction in cloud cover in Long et al. (2009), Augustine and Dutton (2013), and their results are based on data alone.

Authors response: Long et al is equivocal about it, certainly in comparison to Augustine and Dutton. At this point in the text it is inappropriate to include these references because this paragraph deals with European data. We inserted the references at the end of the next paragraph though where more general comment are made.

Why mention that climate models are not capable of reproducing these trends. Are climate models even capable of resolving the cloud physics necessary to resolve the various cloud types and cloud cover responsible for dimming and brightening? I doubt it.

Authors response: On balance a fair point: The paper hardly discusses models so we remove the reference to Allen.

l. 36-42 Wang et al. (2013) has clearly shown that errors associated with single black detector pyranometer measurements adversely affect trends in solar radiation. In this respect, GEBA data are not of unmistakable quality.

Authors response: we adjusted the sentence to:

GEBA data can be used to good effect because of the fact that many stations have submitted data, but the peculiarities of the radiative signals typical to individual localities are invariably lost in the abundance of data.

l. 73-73 Does your statement that cloud cover data are collected simultaneously with radiation data apply to the Netherlands? That may not be true for most of the radiation stations over the globe.

Authors response: True enough, in that sense the Netherlands may indeed be the exception. The statement was adjusted to:

Also, data on fractional cloudiness needs to be collected simultaneously with radiation data.

I. 105 Define acronyms

Authors response: Done

I. 132-133 How is a representative cosine of the solar zenith angle (SZA) determined for a particular hour? Do you use the $\cos(\text{SZA})$ at the midpoint of the hour or do you average the SZAs within the hour period? Averaging SZAs at low sun does not provide a good “representative” SZA for the hour.

Authors response: We use mid-point of the hour which is now stated in the text. [in the appendix]

I. 199 Change “to suggesting that” to “that suggests”

Authors response: Done

I. 220-221 To get proxy data for $\text{Scj}(\text{yk})$ I assume that you plot the data corresponding to the variables in eq. 15 in a way analogous to Langley plots, and then use the resulting relationship to generate the proxy data per okta. Correct? If so, I assume that the scatter, and thus uncertainty, of those plots would be small for clear-sky data and larger for oktas 1 through 8. Those uncertainties would define the error in the various terms of eq. 21. Were those uncertainties incorporated into your analysis? They should at least be presented in some form — if possible. If my interpretation of your proxy data generation is wrong, please better explain your method in the paper.

Authors response:

Yes, thank you for bringing this point to the fore. Scattering and thus uncertainty is larger for higher fractional coverage. We include that in the text (see below). The rest of Ref #2's statement is a rather complicated point though, as for the trend analysis we mix uncertainties in the data points with natural atmospheric variability on a multi-year time scale. The M-K test does not separate these; it simply uses the given data to derive trends. So it will be hard to satisfy Ref #2's comments completely. We experimented with other types of trend analysis than the M-K including one whereby the trend was calculated by randomly imposing errors of a specified value on the data points and recalculating the trends and thus their uncertainties. We got very similar results as our M-K analysis. As the M-K analysis is a standard test of significance used in this type of study we prefer to keep it in (see for example Long et al, 2009). Nevertheless it may be of use to clarify certain parts of the text. Therefore:

We included in the appendix several extra statement explaining the function B and the errors involved:

The parameters α and β are constants determined by fitting the data. The method expressed in Eq (A18) is equivalent to the Langley method of obtained optical thickness with the only difference the weak dependence of B on sun angle. Such dependence is necessary to include because the diffuse radiation arriving at the surface is weakly dependent upon μ_0 ,

And a little lower in the appendix:

Eq (A19) expresses the dependence of atmospheric optical thickness on μ_0 . Regression fits using Eq. (A19) carries uncertainties into the parameter B and through Eq. (A18) into parameter G and into Eq. (A20). For clear-sky the scatter is small but for skies under (partly) cloudy skies the scatter is larger. The standard 1-sigma uncertainty associated with the clear sky proxy computed in Eq. (A20) is 2-3%, increasing to 8-9 % for high okta values.

And in the main text

Tests of trends will be performed using the standard Mann-Kendall (M-K) (Kendall, 1975) non-parametric test often used in this type of analysis (see f.e. Long et al., 2009). after the time series was first decorrelated. The uncertainty value attached to the trend is a test of significance indicating the 95% confidence interval of the calculated slope line. The uncertainties in trend are due to two factors, namely those in yearly-averaged values of S_p as a result of uncertainties in fitting constants in Eq. (A19) (see Appendix for details) and due to natural variability of a multi-year or even decadal origin. Thus the stated uncertainty in output trend is a mix of both factors.

I. 249 This sentence needs to be reworded.

Authors response: 'Is' was changed into 'it' which clarifies it!

I. 270 The 4th term is shown.

Authors response: Point was also noted by Referee #1. It was remnant of a previous version of this manuscript. It is now corrected.

I. 321 "is" should be changed to "in"

Authors response: Yes, done

I. 355 Since you are discussing aerosol optical depth and cloud optical depth in the same sentence, references to each should be specific. In this case, insert “cloud” in front of “optical depth” on this line.

Authors response: Yes, done

I. 366-368 By “cloud fractional coverage at specific cloud cover,” do you mean the transformation of okta observations to fractional cloud cover? If so, please state this more clearly.

Authors response: An imprecise statement on our part. We corrected:

In our analysis, cloud fraction is obtained in a straightforward manner by counting the hourly cloud data so that the hypothesis that changes in aerosol results in changes in cloud cover can be tested.

I. 414 The sentence beginning with “The SNHT was applied ...” is difficult to understand. What do you mean by “reduced with?” and how does that apply to the a) and b) permutations?

Authors response: Yes, we agree, it was unclear and we changed it:

In the first test each station series was subtracted by the mean of the four other station time series. In the second test each station series was subtracted by the other four station time series separately.

I. 516 What is ERA?

Authors response: An acronym in an acronym, not common but unfortunately not unheard of either in the atmospheric sciences! We expanded it:

the European Centre for Medium Range Weather Forecast’s Re-Analysis project, ERA

I. 537 “b)” should be changed to “2)”

Authors response: Done

I. 555 The sentence beginning with “Cloud amount is increasing...” is counterintuitive. It would benefit by inserting “in solar radiation at the surface” after “overall trend.”

Authors response: Done

I. 560 The large tick marks represent 10 Wm^{-2} .

Authors response: Done

1 |

2 **Impact of aerosols and clouds on decadal trends in all-sky**
3 **solar radiation over the Netherlands (1966 – 2015)**

4

5 Reinout Boers¹, Theo Brandsma¹ and A. Pier Siebesma¹

6

7 ¹KNMI, De Bilt, PO Box 201, Netherlands

8 *Correspondence to:* Reinout Boers (reinout.boers@knmi.nl)

9

Abstract. A 50-year hourly dataset of global shortwave radiation, cloudiness and visibility over the Netherlands was used to quantify the contribution of aerosols and clouds to the trends in yearly-averaged all-sky radiation ($1.81 \pm 1.07 \text{ Wm}^{-2}/\text{decade}$). ~~The trend in all-sky radiation was expressed as a linear combination of trends in fractional cloudiness, clear-sky radiation and cloud-base radiation (radiation emanating from the bottom of clouds). Yearly averaged clear-sky and cloud-base radiation data show large year-to-year fluctuations caused by yearly changes in the occurrence of clear and cloudy periods and cannot be used for trend analysis. Therefore, proxy clear-sky and cloud-base radiations were computed. In a proxy analysis hourly radiation data falling within a fractional cloudiness value are fitted by monotonic increasing functions of solar zenith angle and summed over all zenith angles occurring in a single year to produce an average. All three Stable trends can then be derived computed from the data-proxy radiation data records. The results indicate that trends in all three components contribute significantly to the observed trend in all-sky radiation. Trends (per decade) in fractional cloudiness, all-sky, clear-sky and cloud-base radiation were respectively 0.0097 ± 0.0062 , $1.81 \pm 1.07 \text{ Wm}^{-2}$, $2.78 \pm 0.50 \text{ Wm}^{-2}$, and $3.43 \pm 1.17 \text{ Wm}^{-2}$. A functional expression is derived whereby the trend in (proxy) all-sky radiation is a linear combination of trends in fractional cloudiness, (proxy) clear-sky radiation and (proxy) cloud-base radiation. Trends (per decade) in fractional cloudiness, (proxy) clear-sky and (proxy) cloud-base radiation were respectively 0.0097 ± 0.0062 , $2.78 \pm 0.50 \text{ Wm}^{-2}$, and $3.43 \pm 1.17 \text{ Wm}^{-2}$. To add up to the all-sky radiation the three trends have weight factors, namely the difference between the mean cloud-base and clear-sky radiation, the clear-sky factor (1-fractional cloudiness) and the fractional cloudiness, respectively. Our analysis clearly demonstrates that all three components contribute significantly to the observed trend in all-sky radiation.~~ Radiative transfer calculations using the aerosol optical thickness derived from visibility observations indicate that Aerosol Radiation Interaction (ARI) is a strong candidate to explain the upward trend in the clear-sky radiation. Aerosol Cloud Interaction (ACI) may have some impact on cloud-base radiation, but it is suggested that decadal changes in cloud thickness and synoptic scale changes in cloud amount also play an important role.

1 Introduction

Aerosols and clouds impact the solar radiation reaching the surface by radiative absorption and scattering. Although there have been well-recorded trends in the all-sky radiation all over the globe it has been difficult to precisely attribute such trends to trends in either aerosols or clouds. Wide-spread reductions in all-sky radiation in the 1950 – 1970's ('dimming') have been followed by increases in later decades ('brightening'), especially in Europe (Wild et al., 2005; Wild, 2009). Indeed, a thorough evaluation of all-sky radiation data over Europe (Sanchez-Lorenzo et al., 2015) shows conclusively the distinct dip during the 1970's flanked on either side by an earlier downward trend and a later upward trend. The later upward trends are thought to be the result of ~~regulatory restrictions on emissions of air pollution changes in aerosol content and/or to changes in fractional cloudiness. Yet, modelling of this radiative effect (Allen et al., 2013) by computing the impact of changing emissions of aerosols and aerosol precursors derived from CMIP5 have shown that none of the 13 used models in that study can reproduce observational data.~~

One issue hampering the understanding of records of all-sky radiation is that the impacts of aerosols and clouds need to be derived from a single record at observational sites where additional data for instance from clouds,

were often not present. This has led some investigators to group data into regions and rely either on cloud data from stations in the immediate surroundings or from satellites (or both) to supplement their radiation records (Norris and Wild, 2007). Even though good results on trends in clear-sky radiation can be obtained at sites where direct and solar radiation are recorded at the same time such as Baseline Surface Radiation Network stations (Long and Ackermann, 2000; Long et al., 2009; Wild et al., 2005; Gan et al., 2009), most often an investigator will have to rely on single global radiation data records that are specific to the region of interest (such as Manara et al., 2016) or on data stored in the Global Energy Balance Archive (GEBA) archive. GEBA data ~~are of unmistakable quality, can be used to good effect because of the fact that many stations have submitted data,~~ but the peculiarities of the radiative signals typical to individual localities are invariably lost in the abundance of data. It is therefore of great importance that regional studies are carried out that record the changes in surface radiation in relation to atmospheric parameters that can influence such changes.

In the context of Europe there have been a considerable number of regional studies that focus on trends in global radiation and their attribution, such as in Germany (Liepert and Tegen, 2002; Liepert and Kukla, 1997; Liepert, 1997; Liepert, 2002)), in Germany and Switzerland combined (Ruckstuhl et al., 2008; Ruckstuhl and Norris, 2009; Ruckstuhl et al., 2010), in Estonia (Russak, 2009), in the general Baltic states (Ohvri et al., 2009), in Spain (Mateos et al., 2014), in Norway (Parding et al., 2014), northern Europe in general (Stjern et al., 2009) and in Italy (Manara et al., 2015). Even though there are regional differences the summarized global or all-sky radiation data from Europe combined (Sanchez-Lorenzo et al., 2015) displays a minimum in 1984 – 1985 at the end of a ‘dimming’ period with a subsequent return to higher values. The consensus about the decadal trends in global radiation hides a considerable discourse about the attribution of the radiation trends. Of the parameters of interest when investigating the trends in all-sky radiation namely clear-sky radiation, cloudy-sky radiation and fractional cloudiness, the first two have been difficult to isolate from data and were addressed in only a few studies (Wild, 2010). Yet an increasing number of studies indicate that there are good reasons to believe that Aerosol Radiation Interaction (ARI) is responsible for the rise in all-sky radiation after 1985 (f.e. Philipona et al., 2009; Manara et al., 2016; Ruckstuhl et al., 2008) although the timing of the minimum or intensity cannot be simulated very well using current aerosol emission inventories (Ruckstuhl and Norris, 2009; Liepert and Tegen, 2002; Romanou et al., 2007; Turnstock et al., 2015). About the influence of clouds, the situation continues to be elusive. While it is obvious that clouds are important, the difficulty here is that there are several factors that control their impact. For example there are considerable regional differences in fractional cloudiness (Norris, 2005): fractional cloudiness is constant in Northern Europe (Parding et al., 2014), in Germany before 1997 (Liepert, 1997) well after the minimum in global radiation in 1984, and is declining in the period after 1997 in Switzerland and Germany, at least up to 2010 (Ruckstuhl et al., 2010). Furthermore, cloud optical thickness changes can be the result of changes in microphysics or cloud thickness and current observations are not able to separate the two effects. Nevertheless, modelling and observation studies by Romanou et al. (2007), Ruckstuhl and Norris (2009), Chiacchio and Wild (2010), Liepert (1997), ~~and Liepert and Kukla (1997),~~ Long et al. (2009) and Augustine and Dutton (2009) suggest a definite but mixed role for clouds dynamical as well as microphysical influences impacting the trend in all-sky radiation.

88 Attribution studies using only surface-based observations must rely on supplemental data, namely those of
89 clouds (predominantly fractional cloudiness) and aerosols. ~~Also, Data~~ on fractional cloudiness ~~are need to be~~
90 ~~mostly~~ collected simultaneously with radiation data. Up to the mid-1990 clouds were observed by human
91 observers but since then the role of the observers is taken over by- ceilometers. Apart from occasional sun
92 photometer records (Ruckstuhl et al (2008) data on aerosol are often unavailable. However, recent studies by
93 Wu et al. (2014) and Boers et al. (2015) have shown that it is possible to retrieve useful aerosol optical
94 thickness data from surface visibility records. The principal idea behind both studies is almost 50 years old
95 (Eltermann, 1970; Kriebel, 1978; Peterson and Fee, 1981; and revived by the work of Wang, 2009) and asserts
96 that clear-sky optical thickness is most often caused by aerosols residing in the planetary boundary layer which
97 can be characterized by the optical extinction at 550 nm. This parameter is by definition proportional to the
98 inverse of atmospheric horizontal visibility which in turn is a quantity abundantly observed over at least 50
99 years, often together with observations of radiation.

101 Because of the importance attached to potential attribution of observed regional trends in all-sky radiation to
102 aerosols and / or clouds, we analyze hourly records of radiation, cloudiness and visibility data at five climate
103 stations in the Netherlands for the 50-year period 1966–2015. The two aims of this study are a) to quantify the
104 decomposition of the all-sky flux into its contributing components and compute the decadal trends in the
105 components, and b) to discern the relative importance of aerosols and clouds in shaping the observed trends.

107 The remainder of this paper is organized as follows: Section 2 ~~presents-describes briefly~~ the theory and analysis
108 procedures to obtain clear and cloudy-sky signals from the all-sky data. The procedures combine radiation and
109 cloud coverage data. Equations are ~~derived-given~~ describing the manner in which the all-sky radiation is
110 explicitly dependent upon fractional cloudiness, clear-sky radiation and radiation emanating at cloud-base. The
111 equations are based on elementary principles but we believe that this is the first time that these dependencies are
112 explicitly quantified, although the work by Liepert (1997), Liepert (2002), Liepert and Kukla (2002), and
113 Ruckstuhl et al. (2010) contain elements similar to our work. A full derivation of the equations is presented in
114 the Appendix.

116 In section 3 the data analysis is discussed: all meta-data for all stations recorded between the late 1950's and
117 today were examined in order to better understand the impact of any changes in instruments and location and
118 calibrations on the data. Homogeneity tests were performed to discern any possible discontinuities in the data
119 and to understand whether all climate stations indeed belonged to the same climatological regime. Also attention
120 is given to a break in the cloud observations that occurred in 2002 with the transition from the human observer
121 to the ceilometer. Section 4 show the results. The relative influence of clear-sky radiation, cloudy-sky radiation
122 and fractional cloudiness on the all-sky radiation are shown. Also the relative merits of Aerosol Radiation
123 Interaction (ARI) and Aerosol Cloud Interaction (ACI) in influencing the all-sky radiation are discussed.

125 Section 5 concludes this paper with discussion and conclusions.

2 Method

2.1 Decomposition of all-sky radiation into clear and cloudy sky componentsRadiation data, their proxies and trends

An important aspect of this paper is to quantify the various radiative contributions to the all-sky radiation. It is shown in this subsection that there is an elegant way to do so while invoking a minimum set of assumptions. The radiative contributions arise from skies under clear, partly cloudy or overcast sky conditions. The presence of cloud cover which is recorded simultaneously with the radiation assures that it is possible to quantify these different contributions. Cloud cover is normally recorded in oktas (0-8) so that nine different contributions to the radiation can be identified, which together build up the all-sky radiation.

For each okta value it will be assumed that the observed radiation is a linear combination of clear-sky radiation and radiation emanating from cloud-base, each with cloud fraction weight factors that correspond to the okta value at hand. The result is an equation which casts the all-sky radiation as a function of only three components: 1) the clear-sky radiation, 2) the cloud-base radiation and 3) the fractional cloudiness. Long term changes in cloud type could perhaps affect cloud optical properties (liquid water versus ice water) but their influence on trends is unknown and not studied here. The process to calculate the three components ~~will be~~ is then repeated for each year in the period 1966 – 2015, resulting in three time series. The method thus assures that the relative importance of clear-sky radiation, cloud-base radiation and fractional cloudiness to the trend in all-sky radiation can be quantified.

Unfortunately, as has been shown before (Ruckstuhl et al., 2010) the analysis of trends using real data time series is prone to large errors as periods of cloud and clear sky occur at random times throughout the year. Thus, the year-to-year variations in averages are mostly the result in differences in the selection of solar zenith angles used in constructing yearly averages. In the study of decadal variability that may be attributable to physical causes this is an undesirable side effect so that an alternative method needs to be applied in the trend analysis.

The method we applied is coined an analysis of ‘proxies’. We make use of the fact that for each okta value the observed radiation data can be fitted by a monotonically increasing function of solar zenith angle. The line fit is next evaluated at all hourly solar zenith angles occurring in a single year and averaged. The average proxy radiation data that are thus obtained give a much more stable set of values from which (decadal) trends can be calculated.

If S_k is the yearly averaged all-sky radiation (an observable), then S_{pk} is the yearly averaged all-sky proxy radiation in year y_k . It can be shown that

$$S_{pk} = S_{p,c_0,k}(1 - c_k) + c_k S_{p,cloud,k} \quad (1)$$

where $S_{p,c_0,k}$ is the yearly averaged clear-sky proxy radiation, c_k is the yearly averaged fractional cloudiness and

$$S_{p,cloud,k} = \frac{\sum_{j=1}^8 f_k(c_j) c_j S_{p,cb,c_j,k}}{\sum_{j=1}^8 f_k(c_j) c_j} \quad (2)$$

with $f_k(c_j)$ the fractional occurrence of okta j in a given year k, c_j the fractional cloudiness corresponding to okta j, and $S_{p,cb,c_j,k}$ the cloud-base proxy radiation occurring at okta value j. A full derivation to arrive at Eq. (1) is given in the Appendix.

In summary, The all-sky proxy radiation can be expressed as a linear combination of the clear-sky proxy, and the cloud-base proxy radiation each weighted by their yearly mean coverage. Note that the real all-sky radiation (S_k) and the proxy all-sky radiation (S_{pk}) are different, although they are of course quite close in value. S_k is an observable, S_{pk} is derived from Eq. (1) after its components on the right side are first evaluated. However an *a posteriori* comparison between the two has shown that they agree with each other better with a better than 5% margin.

Using Eq. (1) trends can be calculated using the deviation from the averages over the five decades:

$$S'_{pk} = c'_k (\overline{S_{p,cloud}} - \overline{S_{p,c_0}}) + (1 - \bar{c}) S'_{p,c_0,k} + \bar{c} S'_{p,cloud,k} + c'_k (S'_{cloud,k} - S'_{p,c_0,k}) \quad (3)$$

with

S'_{pk} is yearly deviation of the average over the five decades of the all-sky proxy radiation

c'_k is the yearly deviation of the average over the five decades of the fractional cloud cover

\bar{c} is the average over the five decades of the fractional cloudiness

$S'_{p,c_0,k}$ is the yearly deviation of the average over the five decades of the clear-sky proxy radiation

$\overline{S_{p,c_0}}$ is the average over the five decades of the clear-sky proxy radiation

$S'_{p,cloud,k}$ is the yearly deviation of the average over the five decades of the cloud-base proxy radiation

$\overline{S_{p,cloud}}$ is the average over the five decades of the cloud-base proxy radiation.

The derivation of Eq. (3) is given in the Appendix.

We analyze the trends of time series of global radiation $S(y_k)$ where S is the yearly averaged global radiation, y_k is a year in the period 1966 – 2015 and k is the index of the year. We write $S(y_k)$ as a function of two controlling variables: fractional cloudiness (c) and cosine of solar zenith angle ($\mu_a = \cos(\theta_a)$). Each of these two parameters varies between 0 and 1 (i.e. when the sun is below the horizon the variable μ_a is set to zero).

In the observations from meteorological stations the global radiation comes in discrete values, in our case as hourly averages, 8760 or 8784 values in a year. Each of these hourly averages is thus assigned a specific value of μ_0 . The index i is the bin index of counting over μ_0 . To build up the probability space for μ_0 bins of μ_0 can be selected (for example with width 0.05).

Observations of cloudiness are usually assigned in oktas. Okta values (0 – 8) are associated with specific margins of fractional cloud coverage (see table 1 of Boers et al, 2010). We will designate the fractional cloudiness associated with each okta value as c_j , where $j=0-8$. The bivariate distribution function can then be constructed as

$$p(\mu_0 = \mu_{0ik}, c = c_{jk}) = \frac{N_{ijk}}{N_k} \quad (1a)$$

where N_{ijk} is the number of observations in a single bin and

$$\sum_i \sum_j N_{ijk} = N_k \text{ and } \sum_i \sum_j p(\mu_0 = \mu_{0ik}, c = c_{jk}) = 1 \quad (1b,c)$$

Marginal distribution functions of Eq. (1) are

$$f_c(c_{jk}) = \sum_i p(\mu_0 = \mu_{0ik}, c = c_{jk}) = \frac{\sum_i N_{ijk}}{N_k} = \frac{N_{jk}}{N_k} \quad (2)$$

where $f_c(c_{jk})$ is the fractional occurrence of cloud cover within a specific okta value, and

$$f_{\mu_0}(\mu_{0ik}) = \sum_j p(\mu_0 = \mu_{0ik}, c = c_{jk}) = \frac{\sum_j N_{ijk}}{N_k} = \frac{N_{ik}}{N_k} \quad (3)$$

where $f_{\mu_0}(\mu_{0ik})$ is the distribution of cosines of solar zenith angle. While the distribution $f_{\mu_0}(\mu_{0ik})$ is invariant with time as it is solely dependent on the latitude of the observations, $f_c(c_{jk})$ is varying with time due to yearly and possible decadal trends. Yearly averaged fractional cloudiness $c(y_k)$ is found as the expected value of c of the marginal distribution p_c

$$c(y_k) = \sum_{j=1}^8 c_{jk} f_c(c_{jk}) \quad (4)$$

The yearly averages $S(y_k)$ can be computed as the expected value of S , namely the double summation over all values of c and μ_0 that jointly occur in a single year

$$S(y_k) = \sum_i \sum_j S(\mu_0 = \mu_{0ik}, c = c_{jk}) p(\mu_0 = \mu_{0ik}, c = c_{jk}) \quad (5)$$

Here $S(\mu_0 = \mu_{0ik}, c = c_{jk})$ is the average value of S_k in the bin (i,j,k) .

For each okta class we can derive the distribution of zenith angles as the conditionally sampled bivariate distribution at the specific okta class c_{jk} :

$$f_{\mu_0}(\mu_0 = \mu_{0ik} | c = c_{jk}) = \frac{p(\mu_0 = \mu_{0ik}, c = c_{jk})}{f_c(c_{jk})} \quad (6)$$

We now obtain the yearly averaged global radiation in each okta class as the expected value of the hourly global radiation data sampled conditionally with okta class:

$$S_{c_j}(y_k) = \sum_i S(\mu_0 = \mu_{0ik}, c = c_{jk}) f_{\mu_0}(\mu_0 = \mu_{0ik} | c = c_{jk}) \quad (7)$$

Combining Eq. (5), (6) and (7) yields

$$S(y_k) = \sum_j f_c(c_{jk}) S_{c_j}(y_k) \quad (8)$$

Provided that there are adequate observations of cloudiness to select each observation of global radiation according to the okta class in which it occurs, it is possible to calculate $S_{c_j}(y_k)$ directly from the observations.

The assumption we make at this point is that

$$S_{c_j}(y_k) = (1 - c_{jk}) S_{c_0}(y_k) + c_{jk} S_{cb,c_j}(y_k) \quad (9)$$

where S_{cb} is the cloud base radiation. Although Eq. (9) is a customary approximation, it is almost certainly incomplete as it neglects possible contributions to the flux from three dimensional photon scattering between clouds, in particular when cloud cover is broken. However, to our knowledge no useful correction to Eq. (9) has been published taking such scattering into account. Eq. (9) provides the means to estimate cloud base radiation as all other parameters are known. Inserting Eq. (9) into Eq. (8) with some manipulation and using the definition of Eq. (4) yields the desired result:

$$\begin{aligned} S(y_k) &= S_{c_0}(y_k) [1 - \sum_{j=1}^8 f_c(c_{jk}) c_{jk}] + \sum_{j=1}^8 f_c(c_{jk}) c_{jk} S_{cb,c_j}(y_k) = \\ &= S_{c_0}(y_k) [1 - c(y_k)] + c(y_k) S_{cloud}(y_k) \end{aligned} \quad (10)$$

where

$$S_{cloud}(y_k) = \frac{\sum_{j=1}^8 f_c(c_{jk}) c_{jk} S_{cb,c_j}(y_k)}{\sum_{j=1}^8 f_c(c_{jk}) c_{jk}} \quad (11)$$

The parameter $S_{cloud}(y_k)$ is thus the cloud fraction weighted cloud base radiation. Eq. (10) quantifies the all sky radiation as a function of three variables: namely the clear sky radiation, the weighted cloud base radiation and the fractional cloudiness.

2.3 Proxy radiation

It has long been recognized that $S_{c_j}(y_k)$ has large year to year fluctuations because $p(\mu_0 = \mu_{0ik}, c = c_{jk})$ varies from year to year. Extended periods of cloudiness of certain types that influence $p(\mu_0 = \mu_{0ik}, c = c_{jk})$ are associated with synoptic systems that may occur randomly during the year. This means that trend analysis based on Eq. (7) is subject to large uncertainties that can only be alleviated by collecting data over large areas so that different synoptic systems are sampled at the same time (Liepert, 2002), or by averaging $S_{c_j}(y_k)$ over

several years and then performing trend analysis on the reduced and averaged data set (Liepert and Tegen, 2002)). Over a relatively small region as the Netherlands Eq. (7) is unsuitable to use. In fact Ruckstuhl et al (2010) demonstrated that the use of the radiation data in its pure form would lead to wrong interpretations of trends. To reduce the uncertainty in estimates of $S_{c_j}(y_k)$, in particular when estimating the global radiation under cloudless skies $S_{c_0}(y_k)$ some investigators have resorted to fitting an ‘umbrella’ function of clear-sky radiation over all observations within one year (Long et al, 2009; Ruckstuhl et al, 2010) based for example on discrimination of clear skies by analysis of direct and diffuse radiation. In our formulation the approach of fitting an umbrella function is equivalent to a procedure whereby $S(\mu_0 = \mu_{0ik} | c = c_{0k})$ is fitted by a function $G_{c_{0k}}(\mu_{0ik})$. When we proceed in this way, the parameter $S_{p,c_0}(y_k)$ which is a proxy for $S_{c_0}(y_k)$ is calculated as

$$S_{p,c_0}(y_k) = \sum_i G_{c_{0k}}(\mu_{0ik}) f_{\mu_0}(\mu_{0ik}) \quad (12)$$

This is based on strong theoretical arguments to suggesting that $G_{c_{0k}}(\mu_{0ik})$ is a monotonically increasing function of μ_{0ik} given a specific value of c_j . The use of the marginal distribution $f_{\mu_0}(\mu_{0ik})$ in the summation assures that the entire distribution of cosines of solar zenith angles representative for the location at hand is used in the calculation rather than conditional distribution $f_{\mu_0}(\mu_0 = \mu_{0ik} | c = c_{0k})$ which is highly variable from year to year and for which only a summation over a limited set of observations can be used.

In this paper the approach will be to generalize Eq. (12) to all nine okta values as

$$S_{p,c_j}(y_k) = \sum_i G_{c_{jk}}(\mu_{0ik}) f_{\mu_0}(\mu_{0ik}) \quad (13).$$

In other words we will calculate functions of the type $G_{c_{jk}}(\mu_{0ik})$ for each okta value using the observations at hand.

The notion that the functions $G_{c_{jk}}(\mu_{0ik})$ are monotonic increasing with μ_{0ik} comes from Beer’s Law stating that for a single wavelength only the optical thickness of the atmosphere and μ_{0ik} itself are parameters controlling the change in downwelling radiation with μ_{0ik}

$$S_s = \mu_0 S_e \exp(-\tau / \mu_0) \quad (14)$$

Here S_s is the downwelling radiation at the surface, S_e is the extraterrestrial radiation, and τ is the optical thickness of the atmosphere.

Even though the global radiation is a wavelength integrated quantity, the scattering through the atmosphere consisting of water droplets, ice crystals and aerosols at high relative humidity can in first order be assumed to be conservative. Therefore, it is reasonable to assume that $G_{c_{jk}}(\mu_{0ik})$ has a functional form resembling Eq.

(14). When regressed through data taken over an entire year the fitted line has a parameter akin to the yearly averaged optical thickness of the atmosphere as its sole controlling variable.

Consequently, we will adopt the function

$$G(\mu_0) = \mu_0 A \exp(-B/\mu_0) \quad (15)$$

where B is a parameter depending on μ_0 according to

$$B(\mu_0) = \alpha \mu_0^\beta \quad (16)$$

as the diffuse radiation arriving at the surface is weakly dependent upon μ_0 .

The year-to-year determination of proxies in Eq. (13) is used in this paper as it will yield more stable results than the determination of global radiation using the original Eq. (8). The approach will avoid all seasonal elements and yearly variations that are inherent in the distribution $f_{\mu_0}(\mu_0 = \mu_{0ik} | c = c_{jk})$ due to the yearly variable numbers of μ_{0ik} values necessary to compute the conditionally sampled data. Therefore, the computed trends of proxies will reflect the yearly changing transmission through the atmosphere, which is the purpose of this study.

Parallel to Eq. (10) we can write for the proxy global radiation

$$S_p(y_k) = S_{p,c_0}(y_k)[1 - c(y_k)] + c(y_k)S_{p,cloud}(y_k) \quad (17)$$

where $S_{p,cloud}(y_k)$ is obtained from an equation identical to Eq. (11) with $S_{cb}(y_k)$ replaced by $S_{p,cb}(y_k)$.

In summary, the parameters $S_{p,c_0}(y_k)$, $S_{p,cb}(y_k)$, $S_{p,cloud}(y_k)$ are obtained from the proxy analysis in Eqs. (12)–(16). However, note that $S(y_k) \neq S_p(y_k)$ as the proxy analysis is based on an evaluation of proxy fluxes, not of the ‘real’ fluxes. In the analysis to be performed, however, differences between them turned out to be less than 5%.

2.4 Analysis of trend

Once a time series of proxy radiation values is obtained it is possible to compute trends. As explained in the previous section trends in the observed time series of clear sky and cloudy sky radiation are not very useful due to the year-to-year variability. However, trends in the proxy radiation time series do not suffer from such noise and thus can yield meaningful results. A single equation will be derived for the trend in all sky (proxy) radiation from which it emerges that such trend is the result of three components: a) a trend in fractional cloudiness, b) a trend in clear sky radiation and c) a trend in radiation at cloud base.

To derive trends from the yearly averages (proxy) data we write:

$$c(y_k) = \bar{c} + c'(y_k), S_{p,c_0}(y_k) = \overline{S_{p,c_0}} + S'_{p,c_0}(y_k), S_p(y_k) = \overline{S_p} + S'_p(y_k),$$

$$S_{p,cloud}(y_k) = \overline{S_{p,cloud}} + S'_{p,cloud}(y_k) \quad (19)$$

Here the bar represents an average over 5 decades of the yearly averages, and the primed variables are the yearly deviations from the decadal averages. Inserting into Eq. (17) yields

$$S_p(y_k) = \overline{S_p} + S'_p(y_k) = (1 - \bar{c} - c'(y_k))(\overline{S_{p,c_0}} + S'_{p,c_0}(y_k)) + (\bar{c} + c'(y_k))(\overline{S_{p,cloud}} + S'_{p,cloud}(y_k)) \quad (20)$$

Defining $\overline{S_p} = (1 - \bar{c})\overline{S_{p,c_0}} + \bar{c}\overline{S_{p,cloud}}$ and collecting terms yields

$$S'_p(y_k) = c'(y_k)(\overline{S_{p,cloud}} - \overline{S_{p,c_0}}) + (1 - \bar{c})S'_{p,c_0}(y_k) + \bar{c}S'_{p,cloud}(y_k) + c'(y_k)(S'_{p,cloud}(y_k) - S'_{p,c_0}(y_k)) \quad (21)$$

Eq. (21) is the desired result for the analysis of trends. The first component on the right hand side represents perturbations / trends in fractional cloudiness multiplied by the difference in cloud-base and clear-sky radiation, which is negative. Therefore a positive trend in fractional cloudiness will impact as a negative trend component in building up the all-sky radiation. The second term represents the clear-sky perturbations / trend weighted by the average occurrence of clear skies (in our case approximately 0.32). The third term represents the perturbations / trend in cloud-base radiation weighted by the fractional cloud cover (in our case approximately 0.68). The fourth term not shown here is a cross correlation term which in practice can be neglected.

Eq. (21) explains to a large extent the difficulties in attribution studies of the all-sky radiation. Not only the trends in fractional cloudiness, clear-sky and cloud-base radiation are important, but also their relative weight as determined by the mean fractional cloudiness and the difference between the mean clear-sky and cloud-base radiation. In other words, there are a total of five different factors contributing to the trend in all-sky radiation. For example, when the mean cloud fraction is large, as in northwestern Europe, the impact of the trend in clear-sky radiation on the trend in all-sky radiation will be relatively modest in comparison to the impact of trend in cloud-base radiation. The latter would be weighted by a factor 2 (0.32 versus 0.68) more than the trend in clear-sky radiation (0.32 versus 0.68).

Tests of trends will be performed using the standard Mann-Kendall (M-K) (Kendall, 1975) non-parametric test often used in this type of analysis (see f.e. Long et al., 2009). by the Mann-Kendall test (Kendall, 1975) after the time series was first decorrelated. The uncertainty value attached to the trend is a test of significance indicating the 95% confidence interval of the calculated slope line. The uncertainties in trend are due to two factors, namely those in yearly-averaged values of S_p as a result of uncertainties in fitting constants in Eq. (A19) (see Appendix for details) and due to natural variability of a multi-year or even decadal origin. Thus the stated uncertainty in output trend is a mix of both factors.

2.52.2 Retrieval of aerosol optical thickness

Once the method to decompose the all-sky radiation into its clear-sky and cloudy-sky (proxy) components has been applied and a trend analysis is performed, then it is our goal to seek an answer to the question which processes might be responsible for their long-term change. Although possible long-term changes in the synoptic conditions are a conceivable influence an obvious candidate for exploration of cause is the changing aerosol content of the atmosphere. Aerosol content / concentration was not directly observed but visibility was recorded throughout the period from which aerosol optical thickness was derived.

Aerosol optical thickness is the single most controlling factor in changing clear-sky radiation. A radiative transfer model is used here to calculate the clear-sky radiation as a function of the changing optical thickness. The output was compared to the observed clear-sky radiation. The process whereby aerosol can directly affect clear-sky radiation is denoted as the aerosol direct effect or, using a term used in the IPCC (IPCC, 2013) report, the Aerosol Radiation Interaction (ARI).

Aerosols can also affect the microphysical structure of clouds which in turn affects its radiative structure, a process which is commonly denoted as the aerosol indirect effect, or Aerosol Cloud Interaction (ACI, as using the terminology of IPCC, 2013).

The aerosol optical thickness of the atmosphere (τ_a) is a function of aerosol extinction (σ_a) integrated over the depth of the atmosphere

$$\tau_a = \int_0^h \sigma_a dr = \int_0^h \int_0^r Qn(r)r^2 dr dz \quad (224)$$

where Q is the scattering efficiency and can be obtained from Mie-calculations. The parameter $n(r)$ is the density of the size distribution and r is the radius of the particle. The vertical integration over height z is over the depth of the atmosphere (h) and this yields using the Mean Value Theorem:

$$\tau_a \sim \sigma_{a,mean} H = Q_{mean} N_a H R^2 \quad (235)$$

Here N_a is the concentration of aerosols, R is the mean size of the aerosol particles and H is a scaling depth proportional to the depth of the planetary boundary layer. The proportionality factor includes all vertical variations in aerosol, size distribution and optical properties. Aerosol extinction can be approximated as (Eltermann, 1970; Kriebel, 1978, Peterson and Fee, 1981; Wang et al., 2009)

$$\sigma_{a,mean} = \frac{-\log_e(0.05)}{Visibility} \quad (246)$$

Visibility is a measurable quantity and it provides a means to compute aerosol optical thickness at hourly intervals from standard weather station observations. This procedure has been used to obtain decadal time series

of the aerosol optical thickness over the Netherlands and China (Boers et al, 2015; Wu et al., 2014). ~~Here, a universal climatological value for $H = 1000$ m is used to match the calculations of radiation.~~ We examined the European Center for Medium Range Weather Forecast Reanalysis (ERA) data (Dee et al., 2011) for changes in the planetary boundary layer depth. No indications for changes were found in the course of 50 years and a value of 1000 m was used to reflect conditions over the Netherlands.

2.62.3 Radiative transfer calculations

Variations or trends in solar radiation under cloudless conditions are mostly caused by variations in the optical properties and concentrations of aerosols, the ARI. The principle aim here is to assess whether the variations in optical properties can explain the observed variations ~~is in~~ solar radiation. For this purpose, we used a simple radiation transfer model based on the delta-Eddington two-stream approach, as added complexity in radiative transfer models will not increase the confidence in our results (Boers et al., 1994).

For model calculations, the parameters affecting the radiation are aerosol optical thickness, single scattering albedo, asymmetry parameter and Ångström parameter. Of these four parameters the first two are the most important and only the first one can be obtained from observations. It was attempted to derive the single scattering albedo and its time variation from the aerosol composition in the Netherlands (Boers et al., 2015) but its precise quantification remains elusive due to its uncertain dependence on aerosol composition, wavelength, aerosol hygroscopicity and relative humidity. Thus a constant value of 0.90 was used instead. The results of Boers et al. (2015) indicate that a considerable portion of the reduction in aerosol optical thickness or potential solar brightening can be attributed to the reduction of sulphate aerosols after the 1980's. Even though the nitrate values did increase over the same time, their increases cannot completely counterbalance the decreasing sulphate concentrations. The asymmetry parameter and the Ångström parameter are set to 0.69 and 1.5 respectively to reflect typical aerosol values derived for the Netherlands (Boers et al., 2015).

2.72.4 Solar radiation and aerosol-cloud interaction

Variations or trends in solar radiation emanating from the action of clouds are mostly caused by variations in the cloud fractional coverage and by variations in the optical properties and concentrations of droplets or ice. The two main hypotheses for ACI to operate on cloud properties are formulated below as Hypothesis 1 and 2, in the remainder of this paper referred to as ACI-I, and ACI-II, respectively. ACI-I suggests that variations in cloud optical properties are attributable to variations in aerosol concentration itself. A massive amount of literature has been devoted to this subject, but Twomey (1977) is the first one to describe this effect. It is based on a causal link between changes in aerosol concentration (N_a) and cloud droplet concentration (N_c). These two parameters are not necessarily linearly linked: as the amount of aerosol particles increases, it becomes more and more difficult to raise the supersaturation necessary to activate additional particles. Therefore, N_c and N_a are often related by means of a logarithmic function or a power law with exponent smaller than one (Jones et al., 1994; Gultepe and Isaac, 1995), e.g..

$$N_c \sim N_a^{0.26} \quad (257)$$

Only a limited amount of aerosol particles will be activated to cloud droplets and incipient water droplets all compete for the same amount of water vapor as they grow. This means that the mean size of cloud droplets

decreases as the number of cloud droplets increases. The consequence for the cloud optical thickness (Twomey, 1977) is that :

$$\tau_{c,ACI} \sim H_c N_c^{1/3} \quad (268)$$

Here H_c is the depth of the cloud and $\tau_{c,ACI}$ is the cloud optical thickness attributable to the aerosol aerosol-cloud interaction (ACI-I). Thus, compared to Eq.(235) where the equivalent link between aerosol optical thickness and aerosol number concentration is described the dependence of cloud optical depth to number concentration is much weaker.

Combining Eqs. (257) and (268) with Eq. (235) we find:

$$\tau_{c,ACI} \sim \tau_a^{0.26/3} \quad (279)$$

As the cloud optical thickness τ_c (which is due to the ACI –I and other causes) can be obtained from inverting the cloud-base radiative fluxes ~~obtained from Eq. (13),~~ and τ_a can be obtained from Eqs (237), (248), the validity of the Eq. (279) can be studied.

ACI-II suggests that increasing N_c will result in suppression of precipitation so that cloud life time and cloud fraction is increased (Albrecht, 1989). In our analysis, cloud fractional ~~coverage at specific cloud cover~~ is obtained in a straightforward manner by ~~conditional sampling and counting procedures using the~~ hourly cloud data so that the hypothesis that changes in aerosol results in changes in cloud cover can be tested.

3 Data analysis

3.1 Data sources

We used quality controlled time series of hourly data of surface radiation, cloudiness and visibility which are standard output commonly available to the general public and submitted to the traditional climate data repositories. The surface radiation data consist of 10 second data for shortwave radiation instruments integrated over the hour. To be consistent with most publications on the subject of trends in radiation, the hourly average is taken and expressed in Wm^{-2} . The visibility is recorded at the end of each hour, either by the Human Observer (until 2002) or taken from a Present Weather Sensor (PWS, after 2002). The PWS detects the forward scattering of light emitted by a Near Infrared Light Emitting Diode under an angle of 42°. Cloud cover is observed by the Human Observer until 2002 and represents the last 10 minutes of every hour. After 2002 it is observed by a vertically pointing ceilometer and represents the average of the last 30 minutes of the hour.

A serious concern is that conditional sampling was done on the radiation data in a situation where the observation that represents the condition (namely whether or not clouds are present), was not taken in exactly the same time interval as the observation (radiation) itself. Therefore the conditionally sampled data are an imperfect representation of the true situation. This is particularly true for rapidly changing cloudiness conditions. This issue cannot be rectified. However, in this paper exclusive use is made of yearly averages of

464 conditionally sampled radiation data. For these data, the averaging procedure cancels out data with too much or
465 too few clouds within the hour of the selected radiation data, so that the variability observed in the data will be
466 simply enhanced random noise.

467 3.2 Metadata

468 Table 1 presents the basic metadata of the five principal climate stations in the Netherlands together with the
469 dates when the collection of radiation data started. The station metadata archive was analyzed from which it was
470 apparent that initially the regular maintenance and understanding of instruments was inadequate. Typical
471 problems that needed to be overcome were the build-up of moisture between the concentric glass half-domes,
472 the removal of dust and bird droppings, the horizontal alignment of the instrument and the proper positioning of
473 instruments with respect to shading obstacles such as (growing) trees.

474
475 Apart from these issues, insufficient (re)calibration of the instruments, irregular replacement / rotation of
476 instruments from the instrument pool are the reason that the initial years of observation often yielded data of
477 dubious quality. In the end it was decided to discard all data from the climate stations before the year 1966. The
478 data from the station De Bilt are of acceptable quality from 1961 onwards, in particular since from that year
479 onward radiation was measured by two radiometers that were placed side-by-side. However these earlier data
480 will not be used here because this would induce unacceptable weighting on this station of the radiation average
481 in the five year period prior to the year 1966.

482 3.3 Homogeneity test

483 Even though some investigators have attempted with some success to homogenize and gap-fill their data
484 (Manara et al, 2016) for a small region of the Netherlands with few stations (in our case 5) such a
485 homogenization procedure is unlikely to be successful. The reason is that it carries the risk of replacing real data
486 with bogus data which would weigh heavily on the few data time series available. Nevertheless it is instructive
487 to apply a homogeneity test to understand differences between the time series.

488
489 The five radiation time series were analyzed for statistical homogeneity using the Standard Normal
490 Homogeneity Test (SNHT; Alexanderson, 1986). Instead of applying SNHT directly to each station series, we
491 used relative testing. Relative testing removes the natural variation from a time series (while assuming that
492 natural variation is about the same for all locations), which increases the probability of detecting statistically
493 significant breaks. The SNHT was twice applied to each station series. In the first test each station series was,
494 reduced-subtracted with by (a) the mean of the four other station time series. In the second test-and (b)
495 each station series was subtracted by the other four station time series separately. The latter would reveal a break
496 in the series. Note however that the results yield potential statistical breaks, not real ones.

497
498 The homogeneity testing was applied to the 1966-2015 period. The results indicate that De Bilt data are
499 different from the others in the 1966-1975 period, though a possible inhomogeneity reveals itself only in two of
500 the four relative series. From the metadata there is, however, no reason to doubt the quality of the series of De
501 Bilt in this particular period. In fact of all five stations the instruments at the De Bilt observatory were probably

maintained in the most optimum way. Also, the series of Eelde appears to be high relative to the other four station for the 1966 -1972 period although again from the metadata there is no reason to judge the series of Eelde in this particular period as suspect. Eelde is the most north-easterly station in the Netherlands and data from this station were compared to the most nearby German station with a long radiation time series (Norderney, 1967 – 2015). This comparison indicated that Eelde is homogeneous with Norderney, strongly suggesting that the relative high values of radiation at Eelde in the period 1966 – 1972 are indicative of real atmospheric variability rather than instrumental problems.

A similar homogeneity test was applied to the standard aerosol optical thickness output from the stations based on Eq. (23) and (24) which in turn are based on the visibility observations. No discontinuity was detected at the year 2002 indicating good adjustment procedures from Human Observer to instrument at the transition time. From these tests it emerges that the stations Vlissingen and De Bilt depart the most from the average. Furthermore, when all stations are compared, De Bilt departs the most from the other four. Again these differences can very well imply real differences between station, such as for example may be the result of local differences in air pollution that influence visibility (and thus optical thickness).

For the remainder of the research we decided to use the mean of all five stations for the 1966-2015 period. We studied the sensitivity of the results to leaving out stations and found that even though some details were different, it did not significantly alter any of the findings and conclusions.

3.4 Okta and cloud amount

Even though cloud amount is commonly indicated with the parameter okta, its translation to actual cloud amount as a fraction is necessary for usage in this paper. According to World Meteorological Organization guidelines (WMO, 2008) actual cloud amount should be indicated as one okta in case a single cloud is present in an otherwise completely clear-sky. Similarly, if a single hole exist in an otherwise overcast sky cloud amount should be indicated as seven out of eight. Therefore, a cloud amount of one okta corresponds to a lower cloud amount than expected based on the numerical value of one-eighth. Similarly, a cloud amount of seven-eighth corresponds to a larger value than indicated by its numerical value. Boers et al. (2010) evaluated observed cloud amounts expressed in oktas with fractional cloud amounts derived from all-sky observation of clouds using a Total Sky Imager (an instrument sensitive to radiation in the visible part of the solar spectrum) and using a Nubiscope (an all-sky scanning infrared radiometer). We adhere to the results of their study (their section 2.3, table 1) where for okta 0-8 the following cloud amounts are given (in percentage): 0.00, 6.15, 24.94, 37.51, 50.03, 62.56, 75.18, 95.07, 100.

In the analysis presented in the next section a practical problem occurred in distinguishing between radiation emanating from a completely clear-sky or from a sky with a single cloud but otherwise clear. In the latter case, provided that the cloud does not completely block the direct solar beam, it will be impossible to discern whether the radiative flux would have come from a sky with the okta=0. For this reason it was decided to take data from c=0 and c=1 together and designated the combined data as ‘clear-sky’. A similar argument can be made for the

radiation at the high end of cloudiness. Hence, data from $c=7$ and $c=8$ were lumped together as designating an ‘overcast’ sky.

3.5 Discontinuity in 2002

During the year 2002 the Human Observer was replaced by the Present Weather Sensor for visibility observations and by the ceilometer for cloud observations. While the former transition posed little problems in the analysis of data, such was not the case for the latter. When observing clouds the Human Observer takes into account the full 360-degree view of the horizon. A ceilometer only observes a narrow portion of the sky in vertical direction. Although the half –hour averaging of the cloud observations to some extent compensates for the absence of instantaneous hemispheric information, the two types of observation represent different methods of estimating cloud cover so that the conditional sampling of the radiation is significantly affected. For example, the digital nature of the ceilometer observation results in many more observations in the $c = 0$ (cloudless) and the $c = 8$ (overcast) cloud cover selection bin than obtained from the Human Observer (Boers et al., 2010). As a result, the selectively sampled radiation data in both okta bins will be contaminated by data recorded under fractionally cloudy conditions. Contamination by other okta values is also present for data selected for each of the 1 – 7 okta range but less than for overcast sky conditions. As a result, the selectively sampled radiation data showed distinct discontinuities in 2002.

To account for the discontinuity we decided to apply a so-called quantile-quantile correction to the frequency distribution of cloud coverage from the period after 2002 (during which the ceilometer was operative) and adjust it to the frequency distribution from the period before 2002 (during which the Human Observer was operative). The quantile-quantile correction (Li et al., 2010) is commonly used to adjust distributions of meteorological parameters of numerical models to observed distributions of the same parameters. As a first step cloud cover data (converted from okta to fractional cloudiness, see section 3.4) from the period 2002 – 2015 was smoothed by a Gaussian filter with a half-width of two data points (i.e. two hours). This produced a smooth distribution which, when converted back to okta, yielded a distribution similar but not the same to the okta distribution of the Human Observer. The next step was to do a quantile-quantile correction on the smoothed data. The credibility of a quantile-quantile correction depends on whether it can be assured that the average distribution function as observed by the Human Observer does not change over the break (in case the Human Observer would have made the observations after the break). Although there were some long-term changes in the distribution function before the year 2002 they were small enough to assume the invariance of the distribution function over the break. With the application of the quantile-quantile correction the okta values and hence the fractional cloudiness values after the break assume new / corrected values that are applied as new / corrected discriminators in the selection of the radiative flux.

As a proof of soundness of the procedure we applied the quantile – quantile correction and recomputed the fractional cloudiness as the summation $\sum_1^8 f_i c_i = \bar{c}$ (see discussion beneath Eq. (6A4) in the Appendix) and compared the result to satellite observations derived from successive NOAA-satellites (Karlsson et al, 2017). Figure 1 shows the results.

578

579 The NOAA data (red line) comprises an average over the Netherlands and have been bias-corrected. It is clear
580 that the surface data (black line) which are break-corrected after the year 2002 provides an excellent agreement
581 to the NOAA data when compared to the data which are not-break corrected (blue line). Note also that the data
582 that are not break-corrected show a downward trend in cloudiness while the break-corrected data show an
583 upward trend. These results are thus at odds with observations in Germany close to the Netherlands (Ruckstuhl
584 et al, 2010) where cloud cover seems to be declining at least until 2010.

585 4 Results

586 4.1 Decomposing the all-sky radiative fluxes

587 As a first step in understanding the relative impact of clear and cloudy skies on the all-sky radiative flux it is
588 instructive to examine the manner in which the top-of-atmosphere (TOA) radiative flux is reduced by the
589 various constituents and scattering and absorption mechanisms in the atmosphere (Figure 2). The combined
590 effect of all these processes is responsible for reducing the TOA radiative fluxes down to the observed all-sky
591 radiative flux as indicated by the white line at the bottom of the figure. Figure 2 is a combination of calculations
592 and observations. Observed are the all-sky flux (the white line at the bottom of the Figure) and the clear-sky
593 flux (the white line in the middle). Starting from the top downward, the first reduction of the TOA flux is due to
594 Rayleigh scattering, namely downwards from 274 to 253 Wm^{-2} . Continuing downwards ozone absorption is
595 responsible for a further reduction from 253 to 246 Wm^{-2} . Next water vapor absorption reduces the radiative
596 flux by a further 39 Wm^{-2} from 246 to 207 Wm^{-2} . These three decrements were calculated from inputs from
597 [ERA—the European Centre for Medium Range Weather Forecast’s Re-Analysis project, ERA](#) (for the ozone and
598 water vapor absorption) or surface pressure observations (for the Rayleigh scattering).

599

600 The next reduction is due to the aerosol scattering and absorption which takes the radiative flux further down to
601 the observed clear-sky flux (or more precisely the proxy) from 207 Wm^{-2} to $\sim 170 \text{ Wm}^{-2}$ around 1970 or to ~ 185
602 Wm^{-2} near 2015 with a steady increasing value during the intermediate years. The solid white line in the middle
603 of the plot represents the clear-sky flux. The rest of the reduction from the clear-sky radiative flux to the all-sky
604 flux is entirely due to the action of clouds. The observed clear-sky (proxy) shortwave radiation shows that about
605 13.6 Wm^{-2} has been added to the clear-sky radiation over a period of 5 decades. A trend value at $2.78 \pm 0.50 \text{ W}$
606 $\text{m}^{-2} / \text{decade}$ was calculated. ~~by the Mann-Kendall test (Kendall, 1975) after the time series was first~~
607 ~~decorrelated. The uncertainty value attached to the trend is a test of significance indicating the 95% confidence~~
608 ~~interval of the calculated slope line.~~ The upward trend in clear-sky radiation is thus deemed to be strongly
609 significant. The lower white solid line represents the all-sky radiation which is derived straight from the publicly
610 available climate data sources. It shows considerable short-term variations but overall there is a positive trend.
611 The trend value was calculated as $1.81 \pm 1.07 \text{ W m}^{-2} / \text{decade}$ and is thus also considered significant.

612

613 When comparing the different contributions there are three important points to be considered. First, the
614 combined effects of Rayleigh scattering, ozone and water vapor absorption is constant over time. Even though
615 there is a slight increase in water vapor path over the 50-year period, this is not reflected in any discernable

decrease in radiative flux. Second, despite the absence of any significant trends in the respective radiative reductions they make up a very substantial part of the overall reduction from the TOA radiative flux to the all-sky flux (40 – 50%). Third, the two-pronged action of clouds by 1) blocking part of clear-sky flux in reaching the surface and 2) by scattering radiation inside the clouds is considerably larger than the action of scattering and absorption of radiation by aerosols in reducing the TOA radiative flux. The former ranging from double the latter at the beginning of the period to triple the latter at the end of the period.

Figure 3 shows the measured all-sky radiation and the proxy clear-sky and weighted cloud-base radiation. Linear regression lines (blue) as well as a 21-point Gaussian fit (red) are shown in the figure. There is a weak minimum in all-sky radiation at 1984 which is matched by a minimum in cloud-base radiation near 1982 – 1984. In contrast the clear-sky radiation has an upward trend throughout the entire period. All trend are significant when taken over the entire period.

Figure 4 shows the key result of this paper namely the reconstruction of the trend in the all-sky (proxy) flux out of its three main components as formulated in Eq. (243). Here, the last term, a cross correlation term is not shown on account of its very small yearly values (less than 0.5 W m^{-2}). The black curve shows the variation in all-sky proxy radiation as a function of time. Note again that this function is slightly different from the real all-sky radiation data as its construction is based on the proxy data. Even so, the fluctuations and trends in the proxy data are clearly very close to the fluctuations and trends as observed in the real all-sky data of Figure 3. However, the Gaussian-filtered data indicates that the weak minimum in the original data is replaced by a (close to) constant value in the proxy data. The red curve is the contribution to the trend in all-sky proxy radiation due to the trend in cloud amount. Cloud amount is increasing and as a consequence the contribution to the overall trend in solar radiation is negative. The green line is the contribution to the trend in all-sky proxy radiation as a result of the positive trend in clear-sky proxy radiation, but modulated by the average fraction of time that it is actually clear (32%). The blue line is the contribution to the trend in all-sky radiation as a result of the positive trend in proxy cloud-base radiation. It has a broad minimum, but modulated by the fraction that it is cloudy on average (68%). Each curve represents a perturbation with respect to its average and the large tick marks represent intervals of 10 W m^{-2} .

A number of intermediate conclusions can be drawn at this point:

1. The cloud-base and cloud cover contributing trends are of the same order of magnitude whereas the clear-sky trend contribution is less significant than either one of them.
2. As the mean fractional cloudiness at 0.68 is larger than 0.50, the contribution to the all-sky flux due to a trend in cloud-base radiation has a comparatively larger weight than the contribution of the trend in clear-sky radiation.
3. The increase in cloud cover results in a negative trend contribution to the trend in all-sky (proxy) radiation which thus dampens the strong trend contribution due to the increasing cloud-base proxy radiation. The implication is that clouds have become (optically thinner) but at the same time more frequent, the cause of which is unclear.

4. The short-term variations in all-sky radiation are almost entirely due to the short-term variations in fractional cloudiness.
5. The weak minimum (constant) in all-sky (proxy) radiation is strongly linked to trends in clouds, but not as much to the trend in clear-sky radiation.

Table 2 summarizes the results of the trend analysis. Here, also a subselection is made according to the time period over which trend analysis is performed. Significance is indicated in the last column. Note that both the trends in all-sky radiation and the trend in all-sky proxy radiation are given in the table. The trend in all-sky radiation is simply inferred from the data whereas the trend in all-sky proxy radiation is computed from Eq. (3). Thus, contrary to common notion the trend in measured all-sky radiation cannot be recovered from the trends in proxy data. It is only the all-sky proxy trend that can be recovered from the clear-sky proxy term and the cloud-base proxy term of Eq. (3) and in addition from the fractional cloudiness term of Eq. (3). Note furthermore that the fractional cloudiness term in Eq. (3) is a scaled version of the trend in fractional cloudiness, whereas the other two are scaled versions of the trend in clear-sky proxy radiation and cloud-base proxy radiation.

Inspection of the table indicates that none of the trends (including those of the clear-sky proxy radiation) is significant in the period 1966 – 1984. All significant trends occur in the period 1984 – 2015. Two-thirds of the strong upward trend in cloud-base proxy radiation is offset by the cloud fraction trend term in the same period. To our knowledge these calculations are the first of their kind and demonstrate the relative importance of the impacts of clear and cloudy skies on the all-sky radiation. Trend values for the all-sky radiation all fall within the bounds of ~~Lorenzo-Sanchez-Lorenzo~~ et al. (2015) given by their comprehensive summary of Europe's observations. For the clear-sky proxy radiation the trend is positive throughout the entire period and the absence of a curvature matching that of the all-sky radiation does not suggest a very strong causal link with it. In contrast the curvature of the cloud-base proxy radiation curve much more resembles that of the all-sky radiation. Because the fractional cloud cover term partly compensates the strong upward trend of the cloud-base curve after 1985, it strongly suggests that for the Netherlands cloud processes are the dominant factor that impact the shape of the all-sky radiation time series.

4.2 Aerosol-radiation interaction (ARI)

To investigate the possibility of aerosol-radiation interaction the median aerosol optical thickness is derived from the visibility observations. Next radiative transfer model calculations were performed to compute the solar radiation. Figure 5 shows the time series of median aerosol optical thickness for the Netherlands. To about 1985 the optical thickness has a weakly downward trend albeit that there are considerable year-to-year variations. After 1985 there is a distinct downward trend that remains present until the end of the time series in 2015. Overall trend is -0.032 per decade and is significant.

Figure 6 shows the results from radiative transfer computation compared to the clear-sky flux. The solid black and accompanying shading represents the best fit through the data (the points connected by a black line). The blue line is the result of calculating the clear-sky radiation using the aerosol optical thickness in Figure 5 as an input, with a fixed value of the single scattering albedo of 0.90. The calculations indicate a remarkable

694 agreement with the observed clear-sky radiation. The blue line falls entirely within the shaded area of
695 uncertainty of the slope through the data.

696

697 The accuracy of the modeled radiation curves is dependent upon the accuracy of the optical thickness derived
698 from the visibility observations and the value of the single scattering albedo. If the scaling depth used to match
699 the optical thickness observations to satellite and surface-base radiation data (Boers et al., 2015) is changed, so
700 will the position of the model output (blue line) change with respect to the clear – air data ($\delta SW = 5 - 6 \text{ W m}^{-2}$
701 for $\delta \tau = -0.1$).

702

703 There is however no useful information on the time-dependence of the single scattering albedo, the mean value
704 of which is not clear either. The value of 0.90 as used here reflects a compromise between the necessity of
705 having to assign it a value less than one due to the presence of radiation absorbing aerosols (Black Carbon and
706 Organic Aerosols), and the prevalence of pure scattering aerosols in an environment of high relative humidity
707 (sulfates and nitrates) which tend to keep the single scattering albedo at a high value.

708

709 However, the overall conclusion is that the reduction in aerosol concentration resulting in a reduction in aerosol
710 optical thickness is a very strong candidate cause explaining the overall increase in clear-sky solar radiation.
711 This implies that there is a compelling argument that ARI i.e. the direct aerosol effect is responsible for the
712 decadal change in clear-sky radiation.

713 4.3 Aerosol-cloud interaction (ACI)

714 Concerning ACI-I we plotted the left and right sides of the function described in Eq. (279). Here (Figure 7) the
715 cloud optical thickness for clouds has been derived from the monotonic relationship between solar radiation and
716 cloud optical thickness and using the mean weighted cloud-base radiation (bottom curve in Figure 2) as the
717 radiative input. The cloud optical thickness that is thus derived constitutes the left side of Eq. (279). The right
718 side of Eq. (279) is based on the aerosol optical thickness data as shown in Figure 5. According to Figure 7,
719 there is indeed an indication that there may be a link between the two optical thicknesses but the regression line
720 has a larger slope than suggested by Eq. (279). This suggests that there may be other mechanisms that play a
721 role in changing the cloud optical thickness. The most likely candidate responsible for these additional changes
722 is a decadal thinning of clouds. However, there is no confirmation by independent data sources suggesting that
723 such thinning has indeed taken place over the course of five decades.

724

725 Under ACI-II cloud amount is governed by precipitation. Here a reduction in aerosols over time would increase
726 the size of cloud droplets, thus enhancing the fall-out of liquid water and thus reducing cloud amount. However,
727 data shown in Figure 1 indicate that cloud fraction is increasing after 1985 when at the same time the aerosol
728 optical thickness decreases. This does not necessarily mean that ACI-II is not operative, but that other factors
729 (such as large scale synoptic changes) at least overwhelm any possible cloud cover changes due to ACI-II.

730

5 Discussion and conclusions

Our derivation of a trend equation for the all-sky radiation shows that there are five parameters that influence the trend, namely 1) a trend in fractional cloudiness, 2) a trend in clear-sky radiation, 3) a trend in cloud-base radiation, 4) the decadal mean of the fractional cloudiness, and 5) the difference between the decadal means of the cloud-base and the clear-sky radiation. It is therefore not surprising that it has been difficult up to now to come up with any firm conclusions about the relative importance of trends in clouds or clear-sky radiation in contributing to the trend in all-sky radiation. This situation is further hampered by difficulties in the derivation of clear-sky and cloud-base radiation, requiring a specialized analysis removing the year-to-year internal fluctuations in radiation estimates. These-They are the results of periodic synoptic conditions that favor certain cloudiness conditions. An analysis of annual means of radiation selected under specific okta values will produce unrealistic results, as noted by Ruckstuhl et al (2010). In order to overcome this last issue we have cast the problem of estimating annual mean radiation in a two-dimensional framework with cloud fraction (okta) and cosine of solar zenith angle as the two controlling variables. A proxy radiation is derived by fitting per okta value a function that is solely dependent upon cosine of zenith angle. Next annual means are computed using the annually constant distribution of cosine values. Stable values of radiation ensue from which trends can be calculated.

Our analysis comprises 50 years of hourly radiation, cloudiness and visibility data at the five principal climate stations in the Netherlands. We summarize the main conclusions of this work.

- 1) The three most important mechanisms reducing the top-of-the-atmosphere radiation to the observed all-sky radiation are absorption of radiation by water vapor, and scattering and absorption by aerosols and clouds. Over the Netherlands the reduction in radiation due to water vapor absorption is actually larger than from aerosol scattering and absorption. However, as there is no trend in water vapor, there is no trend in the all-sky radiation due to trends in water vapor.
- 2) Trends in clear-sky, cloud-base radiation and fractional cloudiness are all important in contributing to the trend in all-sky radiation.
- 3) Over the Netherlands the clear-sky trend is weighted by 0.32 which is one minus the decadal mean fractional cloud cover and the cloudy-sky trend is weighted by 0.68 (i.e. the decadal mean of fractional cloudiness). Therefore, in the Netherlands a trend in cloud-base radiation has double the weight of a clear-sky radiation trend in contributing to the all-sky radiation trend. Thus, in a general sense this means that the actual value of fractional cloudiness, which has a strong regional dependence, exerts a considerable control over the relative importance of clear-sky and cloud-base radiation trends.
- 4) Over the Netherlands the trend in fractional cloudiness is significantly positive in the period after 1985 and because this trend is multiplied by the (negative) difference between the decadal means of cloud-base and clear-sky radiation, it contributes as a negative trend to the trend in all-sky radiation. As the literature suggests (f.e. Norris, 2005) there are significant regional differences in long term trends in cloud cover, so it indicates that strong regional differences will exist in its contribution to the trend in all-sky radiation.
- 5) As found in most studies (see summary of Lorenzo-Sanchez-Lorenzo et al., 2015), a minimum in all-sky radiation is found around 1985. The negative trend of -1.4 Wm^{-2} up to 1985 is weaker than the

average of Europe (-2.5 Wm^{-2}). The upward trend from 1985 onwards of 2.3 Wm^{-2} is also weaker than the average of Europe (3.2 Wm^{-2}).

- 6) The minimum in all-sky radiation is not matched by a corresponding minimum in clear-sky proxy radiation. An increasing trend of 1.22 Wm^{-2} is found over the earlier period which increased to 3.40 Wm^{-2} later on. After significant amounts of local natural gas were found in the late 1950s the Netherlands were a very early (1960 – 1965) adapter to cleaner fuels which may explain the increase in clear-sky radiation in the earlier period (1966-1985).
- 7) The trend in cloud-base radiation has a similar shape as that of the all-sky radiation. It is weakly negative before 1985 (-0.77 Wm^{-2}) and strongly positive thereafter (4.94 Wm^{-2}). Consequently, the conclusion is justified that the curvature /weak minimum in all-sky radiation around 1985 is caused mostly by the cloud-base radiation.
- 8) As our techniques are able to isolate the clear-sky radiative component it has been possible to study the attribution of changes in aerosol content to the observed trend in clear-sky radiation. Radiative transfer calculations demonstrate that the increase in clear-sky radiation can be completely explained by a concomitant decrease in aerosol optical thickness. This strongly suggests that the ARI (the direct aerosol effect) is a prime candidate to explain the observed increase in clear-sky radiation.
- 9) Similarly, ACI-I and ACI-II have been studied to understand their potential impact on the all-sky radiation. Neither is shown to have a dominant contribution to the trend in the overall all-sky flux but the potential influence of ACI-I and ACI-II cannot be ruled out by the data: There may be other influencing mechanisms that mask the impact of ACI-I and ACI-II such as decadal changes in cloud thickness and fractional cloudiness as a result of large-scale synoptic phenomena.

Prerequisite for our method to work is the availability of simultaneous time series of radiation, cloudiness and visibility. The first two are necessary to resolve the difference between clear and cloudy-sky signals in the radiation data, a method which in this paper has been called the determination of ‘proxies’. Additional observations of visibility are necessary to understand the possible influence of aerosols on radiation.

There are a number of ways to improve and/or facilitate this work in the future:

- 1) The practice of observing different parameters simultaneously can be improved by a more optimum consideration of the impact of one parameter on another. For example aerosols and clouds impact radiation, but radiation is recorded as an hourly average, while clouds and visibility parameters are recorded as averages of smaller time intervals. Often these different recording and averaging intervals are based on WMO standards. Yet, they inhibit the analysis and interpretation of their physical links. It would be better if averaging times were standardized more uniformly or if the basic data underlying the averages become available.
- 2) The relative contribution to the all-sky radiation of cloud thickness remains unclear. Therefore, the potential impact of ACI-I and ACI-II cannot be unambiguously quantified. The best way to resolve this issue is by adding observations of clouds using a cloud radar and a cloud lidar. As clouds are largely transparent to radar probing cloud thickness and its long-term variations can thus be derived. Here, super-sites such as those of the Atmospheric Radiation Measurement program and CloudNet, or long -

term data from CloudSat could be of great assistance. Passive radiation data from satellites are less suitable as they only record radiation emanating from the top of clouds or from the layer just beneath cloud top.

- 3) The impact of changes in the single scattering albedo is unclear. This situation is best resolved by direct observations of the single scattering albedo including its wavelength dependence. However, this suggestion only works for future studies as observations of single scattering albedo have hardly been performed in the past. It may be that regional modelling of past aerosol composition and physical and optical properties may alleviate the historical lack of single scattering albedo data.

Appendix A

A1.1 Averaging using real data

Here we provide a full derivation of the analysis leading to Equations (1) and (3) in the main text. The essential elements in this analysis are 1) A transition from ‘real’ data to ‘proxy’ data which constitutes a different way of averaging yearly data, 2) Expressing the all-sky proxy radiation as a linear combination of clear-sky and cloud-base proxy radiation, and 3) A perturbation analysis from which trends can be calculated.

We analyze the trends of time series of global radiation S_k where S is the yearly averaged global radiation and k is the index of a year in the period 1966 – 2015. We write S_k as a function of two controlling variables: fractional cloudiness c and cosine of solar zenith angle $\mu_0 = \cos(\theta_0)$. Each of these two parameters varies between 0 and 1 (i.e. when the sun is below the horizon the variable μ_0 is set to zero).

In the observations from meteorological stations the global radiation comes in discrete values, in our case as hourly averages, 8760 or 8784 values in a year. Each of these hourly averages is thus assigned a specific value of μ_0 , namely the mid-point of the hour. The index i is the bin index of counting over μ_0 . To build up the probability space for μ_0 bins of μ_0 can be selected at the analyst’s discretion (for example with width 0.05).

Observations of cloudiness are usually assigned in oktas. Okta values (0 – 8) are associated with specific margins of fractional cloud coverage (see table 1 of Boers et al, 2010). We will designate the fractional cloudiness associated with each okta value as c_j where $j = 0 – 8$. The yearly bivariate distribution function can then be constructed as

$$p_k(\mu_{0i}, c_j) = \frac{N_{ijk}}{N_k} \quad (\text{A1a})$$

where N_{ijk} is the number of observations in a single bin and

$$\sum_i \sum_j N_{ijk} = N_k \quad \text{and} \quad \sum_i \sum_j p_k(\mu_{0i}, c_j) = 1 \quad (\text{A1b,c})$$

Marginal distribution functions of Eq. (A1a) are

$$f_k(c_j) = \sum_i p_k(\mu_{0i}, c_j) = \frac{\sum_i N_{ijk}}{N_k} = \frac{N_{jk}}{N_k} \quad (\text{A2})$$

where $f_k(c_j)$ is the fractional occurrence of cloud cover within a specific okta value, and

$$f(\mu_{0i}) = \sum_j p_k(\mu_{0i}, c_j) = \frac{\sum_j N_{ijk}}{N_k} = \frac{N_{ik}}{N_k} \quad (\text{A3})$$

where $f(\mu_{0i})$ is the distribution of cosines of solar zenith angle. While the distribution $f(\mu_{0i})$ is invariant with time as it is solely dependent on the latitude of the observations, $f_k(c_j)$ is varying with time due to yearly

and possible decadal trends. Yearly averaged fractional cloudiness c_k is found as the expected value of c of the marginal distribution p_k

$$c_k = \sum_{j=1}^8 c_j f_k(c_j) \quad (A4)$$

The yearly averages S_k can be computed as the expected value of S , namely the double summation over all values of c and μ_0 that jointly occur in a single year

$$S_k = \sum_i \sum_j S_k(\mu_{0i}, c_j) p_k(\mu_{0i}, c_j) \quad (A5)$$

Here $S_k(\mu_{0i}, c_j)$ is the average value of S_k in the bin (i, j, k) .

For each okta class we can derive the distribution of zenith angles as the conditionally sampled bivariate distribution at the specific okta class c_j :

$$f_k(\mu_{0i} | c_j) = \frac{p_k(\mu_{0i}, c_j)}{f_k(c_j)} \quad (A6)$$

We now obtain the yearly averaged global radiation in each okta class as the expected value of the hourly global radiation data sampled conditionally with okta class:

$$S_{c_j, k} = \sum_i S_k(\mu_{0i}, c_j) f_k(\mu_{0i} | c_j) \quad (A7)$$

Combining Eq. (A5), (A6) and (A7) yields

$$S_k = \sum_j f_k(c_j) S_{c_j, k} \quad (A8)$$

Provided that there are adequate observations of cloudiness to select each observation of global radiation according to the okta class in which it occurs, it is possible to calculate $S_{c_j, k}$ and hence S_k directly from the observations.

The assumption we make at this point is that the hourly observation of radiation is a linear combination of a clear-sky term and a cloud-base term, each weighted by their occurrence:

$$S_k(\mu_{0i}, c_j) = S_k(\mu_{0i}, c_0)(1 - c_j) + S_{k, cb}(\mu_{0i}, c_j)c_j \quad (A9)$$

where $S_{k, cb}$ is the cloud-base radiation. Although Eq. (A9) is a customary approximation, it is almost certainly incomplete as it neglects possible contributions to the flux from three-dimensional photon scattering between clouds, in particular when cloud cover is broken. However, to our knowledge no useful correction to Eq. (A9) has been published taking such scattering into account. To produce a yearly average this function is multiplied by the conditional distribution f (from Equation A6) and summed over all observations occurring in the specific okta class:

$$\sum_i S_k(\mu_{0i}, c_j) f_k(\mu_{0i} | c_j) = \sum_i S_k(\mu_{0i}, c_0) f_k(\mu_{0i} | c_j) (1 - c_j) + \sum_i S_{k,cb}(\mu_{0i}, c_j) f_k(\mu_{0i} | c_j) c_j$$

(A10)

We thus find that

$$S_{c_j k} = S_{c_0 k} (1 - c_j) + S_{cb,j,k} c_j + R_1 \quad (A11a)$$

with

$$R_1 = \sum_i S_k(\mu_{0i}, c_0) [f_k(\mu_{0i} | c_j) - f_k(\mu_{0i} | c_0)] (1 - c_j) \quad (A11b)$$

And

$$S_{cb,j,k} = \sum_i S_{k,cb}(\mu_{0i}, c_j) f_k(\mu_{0i} | c_j) \quad (A11c)$$

In (A11c) all cloud base radiation in a single okta class is simply lumped together. We now calculate the total radiation:

$$S_k = \sum_j S_{c_j k} \quad (A12a)$$

With further manipulation we then find that

$$\begin{aligned} S_k &= S_{c_0 k} [1 - \sum_{j=1}^8 f_k(c_j) c_j] + \sum_{j=1}^8 f_k(c_j) c_j S_{cb,c_j k} + \\ &\sum_j f_k(c_j) \sum_i S_k(\mu_{0i}, c_0) [f_k(\mu_{0i} | c_j) - f_k(\mu_{0i} | c_0)] \quad (A12b) \\ &= S_{c_0 k} [1 - c_k] + c_k S_{cloud,k} + \sum_j \sum_i S_k(\mu_{0i}, c_0) f_k(c_j) [f_k(\mu_{0i} | c_j) - f_k(\mu_{0i} | c_0)] \end{aligned}$$

from which it follows that

$$S_k = S_{c_0 k} [1 - c_k] + c_k S_{cloud,k} + R_2 \quad (A13a)$$

$$R_2 = \sum_j \sum_i S_k(\mu_{0i}, c_0) f_k(c_j) [f_k(\mu_{0i} | c_j) - f_k(\mu_{0i} | c_0)] \quad (A13b)$$

Here

$$S_{cloud,k} = \frac{\sum_{j=1}^8 f_k(c_j) c_j S_{cb,c_j k}}{\sum_{j=1}^8 f_k(c_j) c_j} \quad (A14)$$

The rest terms R_1 and R_2 stem from the fact that the average value S_{c_0k} (A11a) is different for individual okta classes as the summation is done over values of the cosine of solar zenith angle that are different for each okta class. Nevertheless it is expected that both terms are small as the summations in R_1 and R_2 are done over small terms that are positive as well as negative and thus will partly cancel. The parameter $S_{cloud,k}$ is the cloud-base radiation weighted by cloud fraction.

A1.2 Averaging using proxy data

It has long been recognized that S_{c_jk} has large year-to-year fluctuations because $p_k(\mu_{0i}, c_j)$ varies from year-to-year. Extended periods of cloudiness of certain types that influence $p_k(\mu_{0i}, c_j)$ are associated with synoptic systems that may occur randomly during the year. This means that trend analysis based on Eq. (A13) will be subject to large uncertainties that can only be alleviated by collecting data over large areas so that different synoptic systems are sampled at the same time (Liepert, 2002), or by averaging S_{c_jk} over several years and then performing trend analysis on the reduced and averaged data set (Liepert and Tegen, 2002)). Over a relatively small region as the Netherlands Eq. (A13) is unsuitable to use. In fact Ruckstuhl et al (2010) demonstrated that the use of the radiation data in its pure form would lead to wrong interpretations of trends. To reduce the uncertainty in estimates of S_{c_jk} , in particular when estimating the global radiation under cloudless skies S_{c_0k} some investigators have resorted to fitting an ‘umbrella’ function of clear-sky radiation over all observations within one year (Long et al, 2009; Ruckstuhl et al, 2010) based for example on discrimination of clear skies by analysis of direct and diffuse radiation. In our formulation the approach of fitting an umbrella function is equivalent to a procedure whereby $S_k(\mu_{0i}|c_0)$ is fitted by a function $G_{c_0k}(\mu_{0i})$. When we proceed in this way, the parameter S_{p,c_0k} which is a proxy for S_{c_0k} is calculated as

$$S_{p,c_0k} = \sum_i G_{c_0k}(\mu_{0i}) f(\mu_{0i}) \quad (A15)$$

There are strong theoretical arguments to suggest that $G_{c_0k}(\mu_{0i})$ is a monotonically increasing function of μ_{0ik} given a specific value of c_j . The use of the marginal distribution $f(\mu_{0i})$ in the summation assures that the entire distribution of cosines of solar zenith angles representative for the location at hand is used in the calculation rather than conditional distribution $f_k(\mu_{0i}|c_0)$ which is highly variable from year-to-year and for which only a summation over a limited set of observations can be used.

In this paper the approach will be to generalize Eq. (A15) to all nine okta values as

$$S_{p,c_jk} = \sum_i G_{c_jk}(\mu_{0i}) f(\mu_{0i}) \quad (A16)$$

In other words we will calculate functions of the type $G_{c,jk}(\mu_{0i})$ for each okta value using the observations at hand.

The notion that the functions $G_{c,jk}(\mu_{0i})$ are monotonic increasing with μ_{0i} comes from Beer's Law stating that for a single wavelength only the optical thickness of the atmosphere and μ_{0i} itself are parameters controlling the change in downwelling radiation with μ_{0i}

$$S_s = \mu_0 S_e \exp(-\tau / \mu_0) \quad (A17)$$

Here S_s is the downwelling radiation at the surface, S_e is the extraterrestrial radiation, and τ is the optical thickness of the atmosphere.

Even though the global radiation is a wavelength-integrated quantity, the scattering through the atmosphere consisting of water droplets, ice crystals and aerosols at high relative humidity can in first order be assumed to be conservative. Therefore, it is reasonable to assume that $G_{c,jk}(\mu_{0i})$ has a functional form resembling Eq. (A17). When regressed through data taken over an entire year the fitted line has a parameter akin to the yearly averaged optical thickness of the atmosphere as its sole controlling variable.

Consequently, we will adopt the function

$$G(\mu_0) = \mu_0 A \exp(-B / \mu_0) \quad (A18)$$

where B is a parameter depending on μ_0 according to

$$B(\mu_0) = \alpha \mu_0^\beta \quad (A19)$$

The parameters α and β are constants determined by fitting the data. The method expressed in Eq (A18) is equivalent to the Langley method of obtained optical thickness with the only difference the weak dependence of B on sun angle. Such dependence is necessary to include because the diffuse radiation arriving at the surface is weakly dependent upon μ_0 .

Following the procedure outlined for the real data exactly but including the subscript p to indicate 'proxy' and changing the conditional distributions (A6) with the marginal distribution (A3) we can finally write for the proxy global radiation

$$S_{pk} = S_{p,c_0k} (1 - c_k) + c_k S_{p,cloud,k} \quad (A20)$$

where $S_{p,cloud,k}$ is obtained from an equation identical to Eq. (A9) with $S_{cb,k}$ replaced by $S_{p,cb,k}$. Note however that the rest terms R_1 and R_2 have vanished in the proxy formulation. The reason is that the conditional distributions have been replaced by the marginal distribution of cosine of solar zenith angles, which is independent of cloud cover fraction and time. Therefore the marginal distributions in the rest term are all identical and thus will cancel exactly. Equation (A20) is represented in the main text as Eq. (1).

Eq. (A19) expresses the dependence of atmospheric optical thickness on μ_0 . Regression fits using Eq. (A19) carries uncertainties into the parameter B and through Eq. (A18) into parameter G and into Eq. (A20). For clear-sky the scatter is small but for skies under (partly) cloudy skies the scatter is larger. The standard 1-sigma uncertainty associated with the clear sky proxy computed in Eq. (A20) is 2-3%, increasing to 8-9 % for high okta values.

The year-to-year determination of proxies in Eq. (A20) is used in this paper as it will yield more stable results than the determination of 'true' averages. The approach will avoid all seasonal elements and yearly variations that are inherent in the distribution $f_k(\mu_{0i}|c_j)$ due to the yearly variable numbers of μ_{0i} values necessary to compute the conditionally sampled data. Therefore, the computed trends of proxies will reflect the yearly changing transmission through the atmosphere, which is the purpose of this study.

Note finally that $S_k \neq S_{pk}$ as the proxy analysis is based on an evaluation of proxy fluxes, not of the 'real' fluxes. In the analysis to be performed, however, differences between them turned out to be less than 5%.

A1.3 Analysis of trend

Once a time series of proxy radiation values is obtained it is possible to compute trends. As explained in the previous section trends in the observed time series of clear-sky and cloudy sky radiation are not very useful due to the year-to-year variability. However, trends in the proxy radiation time series do not suffer from such noise and thus can yield meaningful results. A single equation will be derived for the trend in all-sky (proxy) radiation from which it emerges that such trend is the result of three components: a) a trend in fractional cloudiness, b) a trend in clear sky radiation and c) a trend in radiation at cloud-base.

To derive trends from the yearly averages (proxy) data we write:

$$c_k = \bar{c} + c'_k, S_{p,c_0,k} = \bar{S}_{p,c_0} + S'_{p,c_0,k}, S_p(y_k) = \bar{S}_p + S'_p(y_k), S_{p,cloud,k} = \bar{S}_{p,cloud} + S'_{p,cloud,k} \quad (A21)$$

Here the bar represents an average over 5 decades of the yearly averages, and the primed variables are the yearly deviations from the averages over the five decades under analysis. Inserting into Eq. (A20) yields

$$S_{pk} = \bar{S}_p + S'_{pk} = (1 - \bar{c} - c'_k)(\bar{S}_{p,c_0} + S'_{p,c_0,k}) + (\bar{c} + c'_k)(\bar{S}_{p,cloud} + S'_{p,cloud,k}) \quad (A22)$$

Defining $\bar{S}_p = (1 - \bar{c})\bar{S}_{p,c_0} + \bar{c}\bar{S}_{p,cloud}$ and collecting terms yields

$$S'_k = c'_k(\bar{S}_{p,cloud} - \bar{S}_{p,c_0}) + (1 - \bar{c})S'_{p,c_0,k} + \bar{c}S'_{p,cloud,k} + c'_k(S'_{p,cloud,k} - S'_{p,c_0,k}) \quad (A23)$$

Eq. (A23) can be used for trend analysis and is represented in the main text as Eq. (3).

1007 The implications of this expression are quite important. Eq. (A23) demonstrates that the trend in all-sky
1008 radiation is not a simple summation of trends in clear-sky and cloudy-sky trends, which would perhaps be an
1009 intuitive notion when seeking to explain the observed trend in all sky radiation. Eq. (A23) demonstrates that a)
1010 the trends in clear-sky and cloud-base radiation need to be weighted by their fractional occurrence in the
1011 atmosphere, and that b) there is a third term constituting the trend in fractional cloudiness scaled by the
1012 difference in average cloud-base and clear-sky radiation. Furthermore, the additional fourth term, which is
1013 shown to be negligible in the current analysis, may not always be small when there are significant cross
1014 correlations between the perturbations.

1016 **Data availability**

1017 The data used in this paper can be downloaded from the KNMI website:

1018 <http://www.knmi.nl/nederland-nu/klimatologie/uurgegevens>

1019

1020 **Acknowledgments**

1021 We acknowledge the use of EUMETSAT's CMSAF cloud climatology data sets. We much appreciated
1022 discussions with Jan Fokke Meirink who made us aware of this data set and who instructed us on its use in this
1023 analysis. We also appreciated discussion with Wiel Wauben about the break analysis.

1024

1025 **Tables**

1026

1027 **Table 1: Details of the stations and the introduction data of the radiometers.**

Station	WMO nr.	LAT (N)	LON (E)	ALT (m)	Introduction date
De Kooy	06235	52.924	4.785	0.5	24 September 1964
De Bilt	06260	52.101	5.177	2.0	10 May 1957
Eelde	06280	53.125	6.586	3.5	2 October 1964
Vlissingen	06310	51.442	3.596	8.0	10 April 1962
Maastricht	06380	50.910	5.768	114.0	5 March 1963

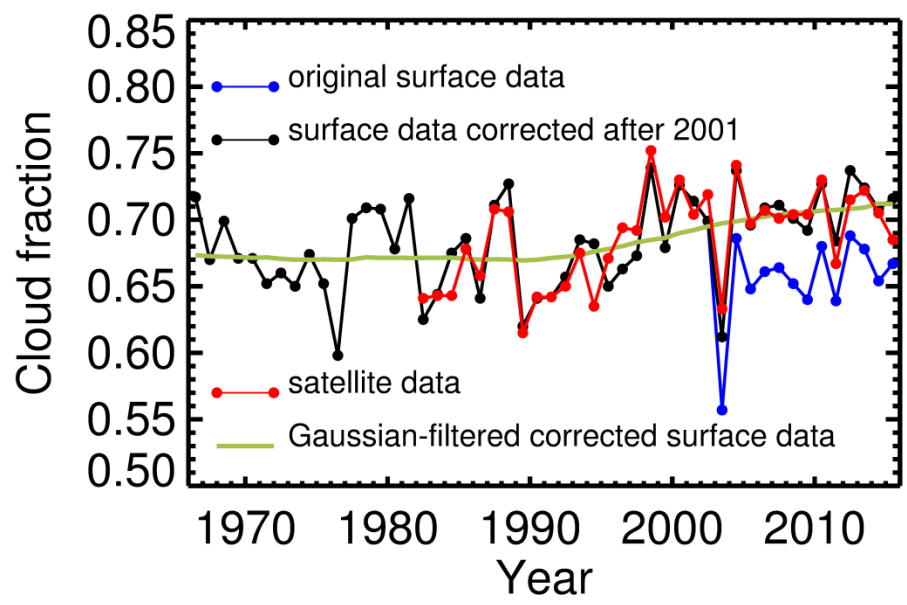
1028

1029

1030 **Table 2. Summary of trend analysis. Except for the fractional cloudiness, all parameters have $W m^{-2} /$**
1031 **decade as a unit. Whether or not the indicated trend is significant is indicated by the star in the column**
1032 **‘uncertainty’.**

Type	Period	Trend	Uncertainty
Fractional cloudiness	1966-2015	0.0097	0.0062*
	1966-1984	-0.0055	0.0344
	1984-2015	0.0205	0.0117*
All-sky radiation	1966-2015	1.81	1.07*
	1966-1984	-1.40	4.19
	1984-2015	3.30	1.55*
All-sky proxy radiation	1966- 2015	1.89	0.78*
	1966- 1984	0.39	3.86
	1984- 2015	2.30	1.68*
Clear-sky proxy radiation	1966-2015	2.78	0.50*
	1966-1984	1.22	2.14
	1984-2015	3.46	1.35*
Cloud-base proxy radiation	1966-2015	3.43	1.17*
	1966-1984	-0.77	2.01
	1984-2015	4.94	2.30*
Fractional cloudiness term of Equation (3)	1966-2015	-1.06	0.67*
	1966-1984	0.43	3.30
	1984-2015	-2.22	1.19*
Clear-sky proxy term of Equation (3)	1966-2015	0.88	0.16*
	1966-1984	0.39	0.68
	1984-2015	1.09	0.43*
Cloud-base proxy term of Equation (3)	1966-2015	2.35	0.80*
	1966-1984	-0.53	1.38
	1984-2015	3.37	1.57*

1033



1035

1036 **Figure 1. Surface-based cloud fraction estimates versus satellite-based estimates.**

1037

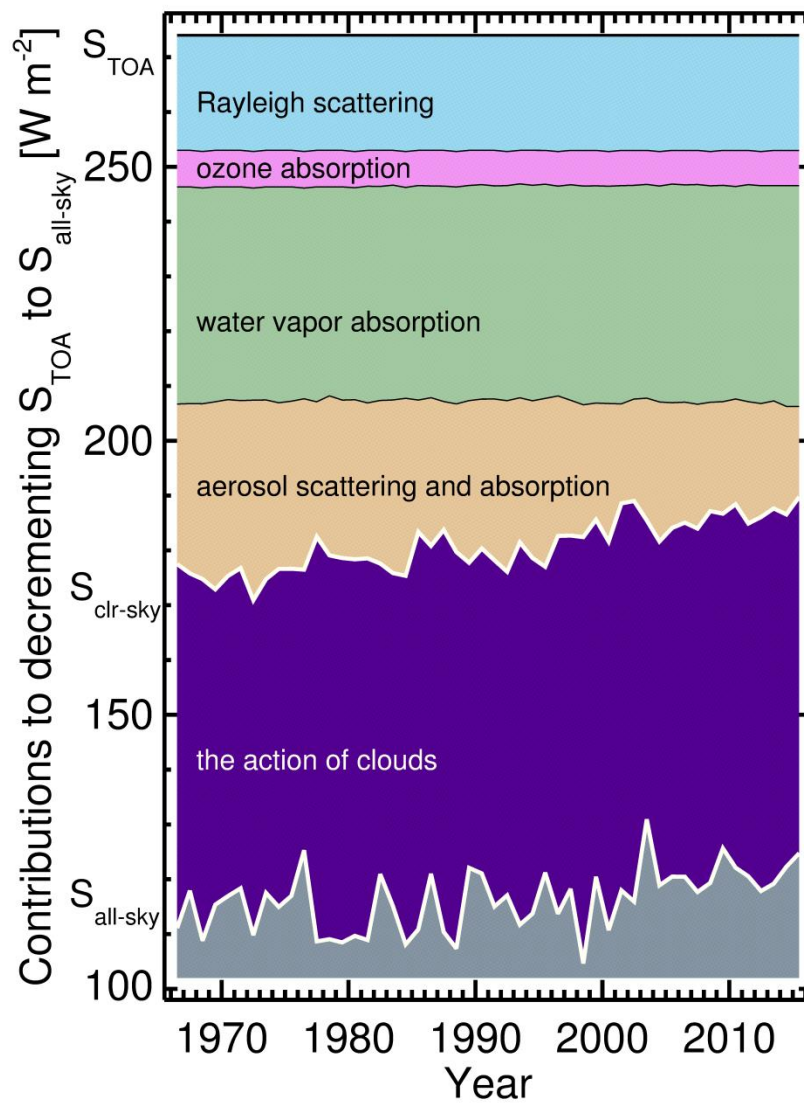


Figure 2. Impact on all-sky flux due to Rayleigh scattering, ozone absorption, water vapor absorption, aerosol scattering and absorption and the action of clouds.

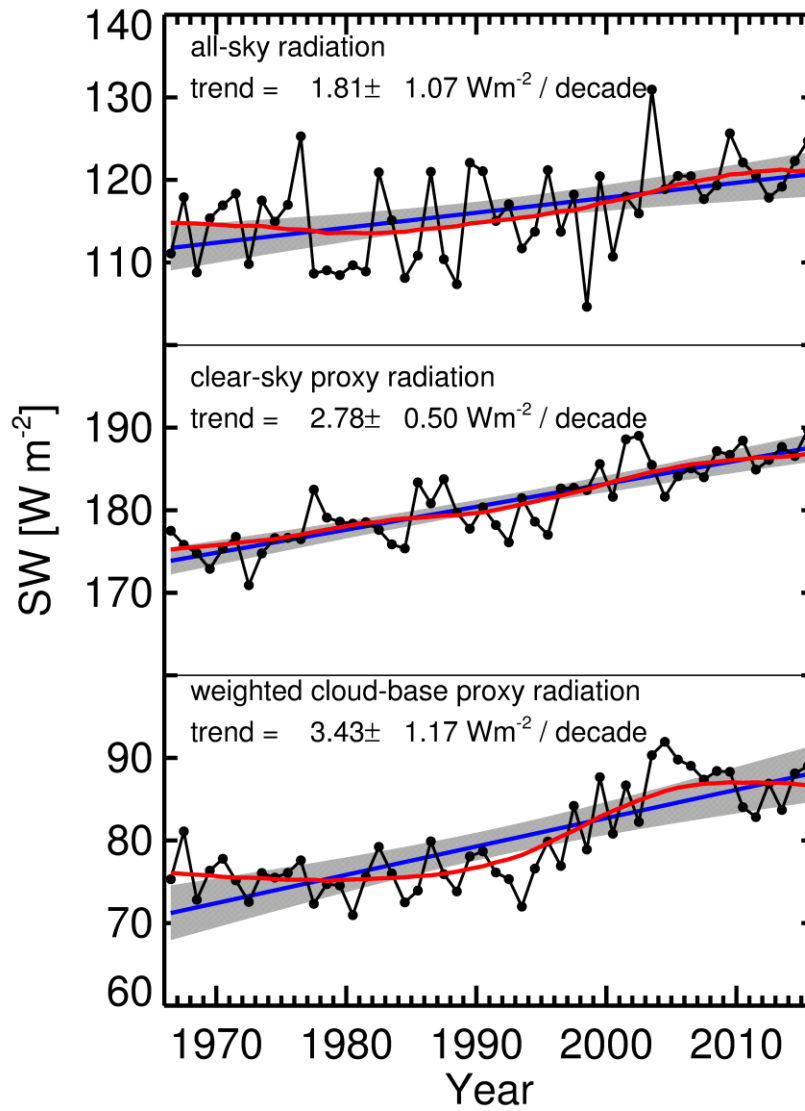
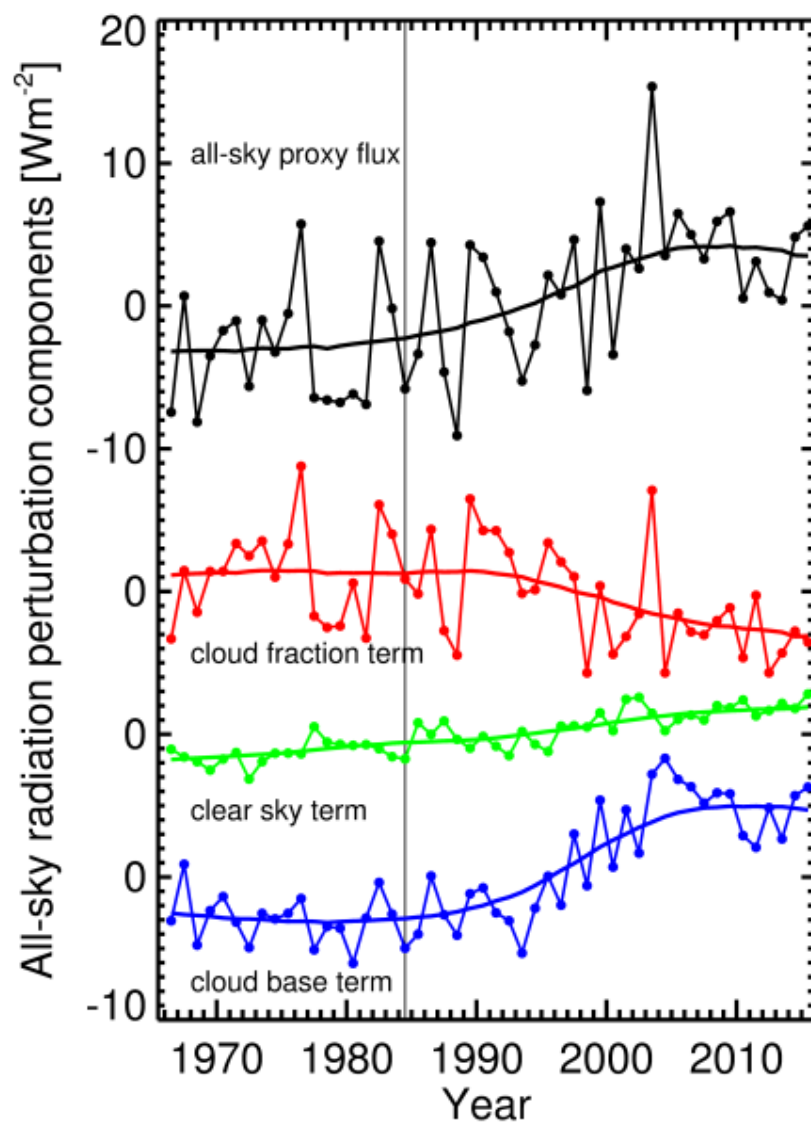


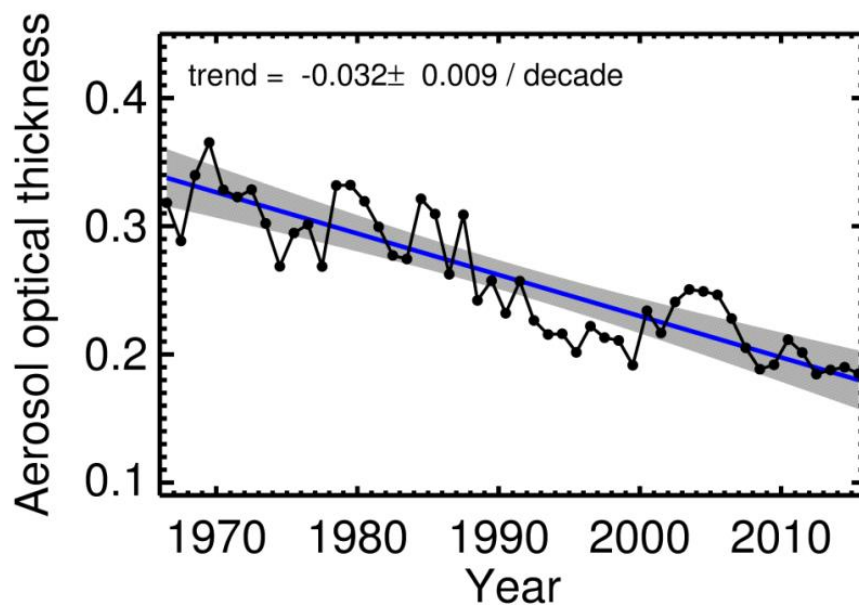
Figure 3. All-sky, clear-sky proxy and cloud-base proxy radiation as a function of time. Blue lines are the regression fits with the grey area as the uncertainty around the fit. The red lines are 21-point Gaussian filter smoothers.



1047

1048 **Figure 4. All-sky radiation perturbation components. Terms are indicated in the graph. 21-point**
 1049 **Gaussian filter smoothers are drawn through the curves.**

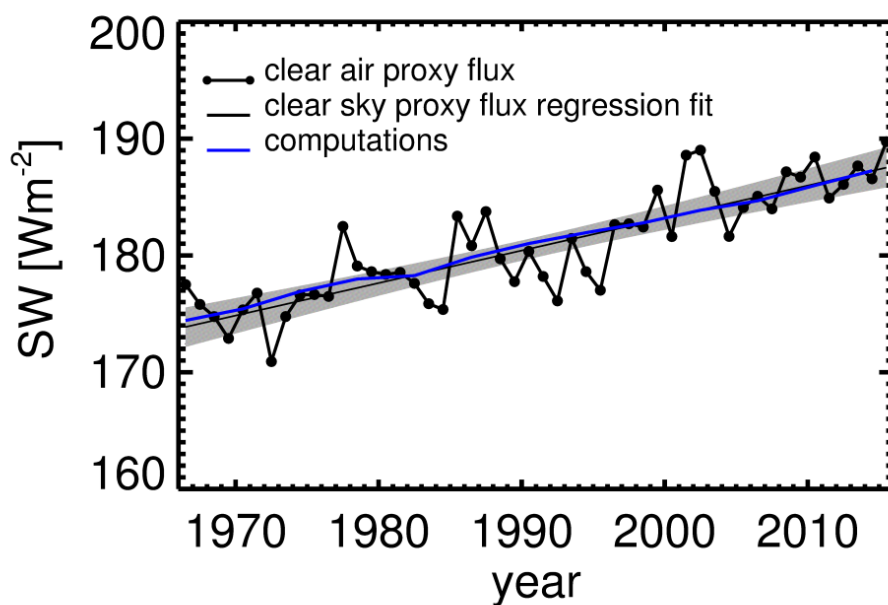
1050



1051

1052 **Figure 5. Aerosol optical thickness derived from visibility observations.**

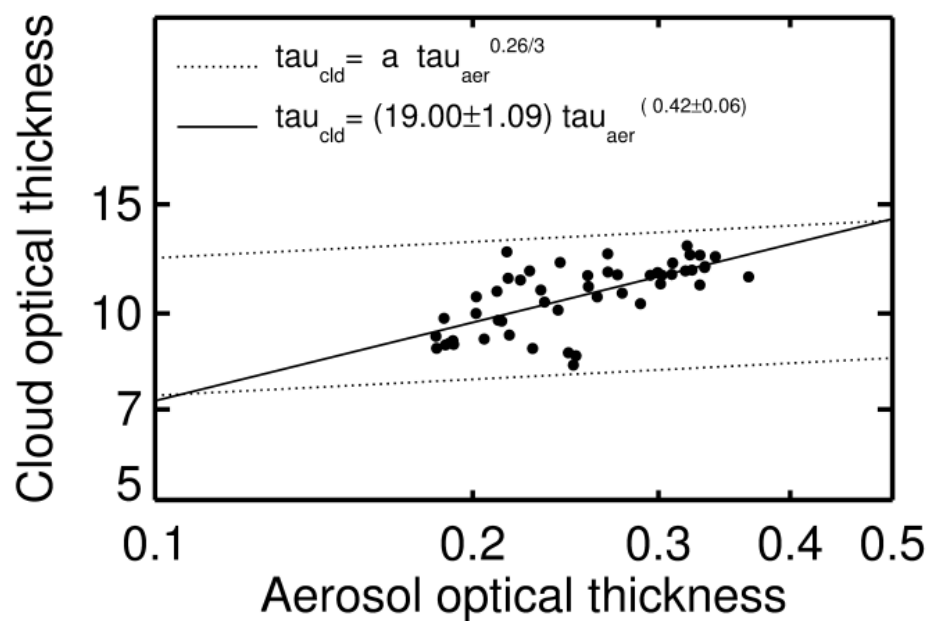
1053



1054

1055 **Figure 6. Clear-sky radiation observations matched by radiative transfer computations.**

1056



1057

1058 **Figure 7. Cloud optical thickness as a function of aerosol optical thickness. The broken lines are the**
 1059 **suggested dependencies of the two optical thicknesses assuming that ACI-I is valid. The solid line is the**
 1060 **actual fit through the data.**

1061

References

- Albrecht, B. A., Aerosols, cloud microphysics and fractional cloudiness, *Science*, 245, 1227 – 1230, 1989.
- Alexanderson H., A homogeneity test applied to precipitation data, *J. of Clim.*, 6, 661-675, 1986.
- [Augustine, J. A. and E.G. Dutton, Variability of the surface radiation budget over the United States from 1996 through 2011 from high-quality measurements, J. Geophys. Res., 118, doi:10.1029/2012JD018551.](#)
- ~~Allen, R. J., J. R. Norris, and M. Wild, Evaluation of multidecadal variability in CMIP5 surface solar radiation and inferred underestimation of aerosol direct effects over Europe, China, Japan, and India, J. Geophys. Res. Atmos., 118, 6311–6336, doi:10.1002/jgrd.50426, 2013.~~
- [Boers, R and R. M. Mitchell, Absorption feedback in stratocumulus cloud: Influence on cloud top albedo, Tellus, 46A, 229 – 241, 1994.](#)
- Boers, R., M. J. de Haij, W. M. F. Wauben, H. K. Baltink, L. H. van Uft, M. Savenije, and C. N. Long, Optimized fractional cloudiness determination from five ground-based remote sensing techniques, *J. Geophys. Res.*, 115, D24116, doi:10.1029/2010JD014661, 2010.
- Boers, R., M. van Weele, E. van Meijgaard, M. Savenije, A.P. Siebesma, F. Bosveld and P. Stammes, Observations and projections of visibility and aerosol optical thickness (1956–2100) in the Netherlands: Impacts of time-varying aerosol composition and hygroscopicity, *Environ. Res. Lett.*, 10, 015003, doi:10.1088/1748-9326/10/1/015003, ~~2014~~[2015](#).
- Chiacchio, M., and M. Wild, Influence of NAO and clouds on long-term seasonal variations of surface solar radiation in Europe, *J. Geophys. Res.*, 115, D00D22, doi:10.1029/2009JD012182, 2010.
- Dee, D. et al., The ERA-Interim reanalysis: configuration and performance of the data assimilation system. *Quart. Journal Roy. Meteor. Soc.*, **137**, 553 – 597, 2010.
- Eltermann, L., Relationships between vertical attenuation and surface meteorological range, *Appl. Optics*, 9, 1804–1810., doi:10.1364/AO.9.001804, 1970.
- Gan, C.-M., J. Pleim, R. Mathur, C. Hogrefe, C. N. Long, J. Xing, S. Roselle, and C. Wei, Assessment of the effect of air pollution controls on trends in shortwave radiation over the United States from 1995 through 2010 from multiple observation networks. *Atmos. Chem. Phys.*, 14, 1701–1715, 2014, [www.atmos-chem-phys.net/14/1701/2014/doi:10.5194/acp-14-1701-2014](#), ~~2014~~, ~~doi:10.5194/acp-14-1701-2014, 2014.~~

1101 Gultepe, I and G. A. Isaac, The relationship between cloud droplet and aerosol number concentration for
 1102 climate models. *Int. J. Climat.* 16, 941 – 946, 1995.

1103

1104 IPCC, Climate Change 2013: The Physical Science Basis. Contribution of Working Group I to the Fifth
 1105 Assessment Report of the Intergovernmental Panel on Climate Change [Stocker, T.F., D. Qin, G.-K. Plattner, M.
 1106 Tignor, S.K. Allen, J. Boschung, A. Nauels, Y. Xia, V. Bex and P.M. Midgley (eds.)]. Cambridge University
 1107 Press, Cambridge, United Kingdom and New York, NY, USA, 1535 pp, doi:10.1017/CBO9781107415324,
 1108 2013.

1109

1110 Jones, A, D. L. Roberts and A. Slingo, A climate model study of indirect radiative forcing by anthropogenic
 1111 sulphate aerosols. *Nature*, 370, 450 – 453, 1994.

1112

1113 Karlsson, K.-G., Anttila, K., Trentmann, J., Stengel, M., Meirink, J. F., Devasthale, A., Hanschmann, T., Kothe,
 1114 S., Jääskeläinen, E., Sedlar, J., Benas, N., van Zadelhoff, G.-J., Schlundt, C., Stein, D., Finkensieper, S.,
 1115 Håkansson, N., and Hollmann, R., CLARA-A2: The second edition of the CM SAF cloud and radiation data
 1116 record from 34 years of global AVHRR data, *Atmos. Chem. Phys. Discuss.*, doi:10.5194/acp-2016-935, ~~in~~
 1117 [review, 2016 revised manuscript accepted for publication in ACP.](#)

1118

1119 Kendall, M.G., Rank Correlation Methods, 4th edition, Charles Griffin, London, 1975.

1120

1121 Kriebel, K. T., On the determination of the atmospheric optical depth by measurements of the meteorological
 1122 range, *Beitr. Phys. Atmos.*, 51, 330, 1978.

1123

1124 Li, H., J. Sheffield, and E. F. Wood, Bias correction of monthly precipitation and temperature fields from
 1125 Intergovernmental Panel on Climate Change AR4 models using equidistant quantile matching, *J. Geophys. Res.*,
 1126 115, D10101, doi:10.1029/2009JD012882, 2010.

1127

1128 Liepert, B. G., Observed reductions of surface solar radiation at sites in the United States and worldwide from
 1129 1961 to 1990, *Geophys. Res. Lett.*, 29, 10, 1421, 10.1029/2002GL014910, 2002.

1130

1131 Liepert. B. G., Recent changes in solar radiation under cloudy conditions in Germany. *Intern. J. climatology* 17,
 1132 1581 – 1593, 1997.

1133

1134 Liepert, B and I. Tegen, Multidecadal solar radiation trends in the United States and Germany and direct
 1135 tropospheric aerosol forcing. *J. Geophys. Res.*, 107, D12, 4153, 10.1029/2001JD000760, 2002.

1136 Liepert, B. and G. Kukla, Decline in solar radiation with increased horizontal visibility in Germany between
 1137 1964 and 1990. *Journal of Climate*, 10, 2391 – 2401, 1997.

1138

1139 Long , C. N., and T. P. Ackerman, Identification of clear skies from broadband pyranometer measurements and
 1140 calculation of downwelling shortwave cloud effects, *J. Geophys. Res.*, 105, D12, 15,609-15, 626, 2000.

1141

1142 Long, C. N., E. G. Dutton, J. A. Augustine, W. Wiscombe, M. Wild, S. A. McFarlane, and C. J. Flynn,
 1143 Significant decadal brightening of downwelling shortwave in the continental United States, *J. Geophys. Res.*,
 1144 114, D00D06, doi:10.1029/2008JD011263, 2009.

1145

1146 Manara, V, M. Brunetti, A. Celozzi, M. Maugeri, A. Sanchez-Lorenzo, and M. Wild, Detection of
 1147 dimming/brightening in Italy from homogenized all-sky and clear-sky surface solar radiation records and
 1148 underlying causes (1959–2013), *Atmos. Chem. Phys.*, 16, 11145–11161, doi:10.5194/acp-16-11145-2016,
 1149 2016.

1150

1151 Mateos, D., A. Sanchez-Lorenzo, M. Antón, V. E. Cachorro, J. Calbó, M. J. Costa, B. Torres, and M. Wild,
 1152 Quantifying the respective roles of aerosols and clouds in the strong brightening since the early 2000s over the
 1153 Iberian Peninsula, *J. Geophys. Res.*, 119, 10,382–10,393, doi:10.1002/2014JD022076, 2014.

1154

1155 Norris, J. R., Multidecadal changes in near-global cloud cover and estimated cloud cover radiative forcing, *J.*
 1156 *Geophys. Res.*, 110, D08206, doi:10.1029/2004JD005600, 2005.

1157

1158 Norris, J. R., and M. Wild, Trends in aerosol radiative effects over Europe inferred from observed cloud cover,
 1159 solar “dimming,” and solar “brightening”, *J. Geophys. Res.*, 112, D08214, doi:10.1029/2006JD007794, 2007.

1160

1161 Ohvri, H., et al., Global dimming and brightening versus atmospheric column transparency, Europe, 1906–
 1162 2007, *J. Geophys. Res.*, 114, D00D12, doi:10.1029/2008JD010644, 2009.

1163

1164 Parding, K., J. A. Olseth, K. F. Dagestadt and B. G. Liepert, Decadal variability of clouds, solar radiation and
 1165 temperature at a high-latitude coastal site in Norway, *Tellus B* 66, 25897, 2014.

1166

1167 Peterson, J. T., and C. J. Fee, Visibility-atmospheric turbidity dependence at Raleigh, North Carolina, *Atmos.*
 1168 *Environ*, 15(12), 2561-2563, 1981.

1169

1170 Philipona, R., K. Behrens, and C. Ruckstuhl, How declining aerosols and rising greenhouse gases forced rapid
 1171 warming in Europe since the 1980s, *Geophys. Res. Lett.*, 36, L02806, doi:10.1029/2008GL036350, 2009.

1172

1173 Romanou, A., B. Liepert, G. A. Schmidt, W. B. Rossow, R. A. Ruedy, and Y. Zhang, 20th century changes
 1174 in surface solar irradiance in simulations and observations, *Geophys. Research Lett.* 34, L057113, doi:
 1175 10.1029/2006GL028356, 2007.

1176

1177 Ruckstuhl, C., and J. R. Norris, How do aerosol histories affect solar “dimming” and “brightening” over
 1178 Europe?: IPCC-AR4 models versus observations, *J. Geophys. Res.*, 114, D00D04, doi:10.1029/2008JD011066,
 1179 2009.

1180

1181 Ruckstuhl, C., J. R. Norris, and R. Philipona, Is there evidence for an aerosol indirect effect during the recent
 1182 aerosol optical depth decline in Europe?, *J. Geophys. Res.*, 115, D04204, doi:10.1029/2009JD012867, 2010.
 1183

1184 Ruckshuhl, C. and R. Philipona, Detection of cloud-free skies based on sunshine duration and on the variation of
 1185 global solar irradiance, *Meteor. Zeitschrift*, 17, No. 2, 181-186, 2008.
 1186

1187 Ruckstuhl, C., R. Philipona, K. Behrens, M. Collaud Coen, B. Durr, A. Heimo, C. Matzler, S. Nyeki, A.
 1188 Ohmura, L. Vuilleumier, M. Weller, C. Wehrli, and A. Zelenka, Aerosol and cloud effects on solar brightening
 1189 and the recent rapid warming, *Geophys. Res. Lett.*, 35, L12708, doi:10.1029/2008GL034228, 2008.
 1190

1191 Russak, V., Changes in solar radiation and their influence on temperature trend in Estonia (1955–2007), *J.*
 1192 *Geophys. Res.*, 114, D00D01, doi:10.1029/2008JD010613, 2009.
 1193

1194 Sanchez-Lorenzo, A., M. Wild, M. Brunetti, J. A. Guijarro, M. Z. Hakuba, J. Calbó, S. Mystakidis, and B.
 1195 Bartok, Reassessment and update of long-term trends in downward surface shortwave radiation over Europe
 1196 (1939–2012), *J. Geophys. Res. Atmos.*, 120, 9555–9569, doi:10.1002/2015JD023321, 2015.
 1197

1198 Stjern, C. W., J.E. Kristjansson and A. W. Hansen, Global dimming and global brightening – an analysis of
 1199 surface radiation and cloud cover data in northern Europe. *Int. J. Climatol.* 29: 643–653, 2009.
 1200

1201 Turnock, S.T., D. V. Spracklen, K. S. Carslaw, G. W. Mann, M. T. Woodhouse, P. M. Forster, J. Haywood, C.
 1202 E. Johnson, M. Dalvi, N. Bellouin, and A. Sanchez-Lorenzo, Modelled and observed changes in aerosols and
 1203 surface solar radiation over Europe between 1960 and 2009 *Atmos. Chem. Phys.*, 15, 9477–9500, [www.atmos-](http://www.atmos-chem-phys.net/15/9477/2015/)
 1204 [chem-phys.net/15/9477/2015/](http://www.atmos-chem-phys.net/15/9477/2015/) doi:10.5194/acp-15-9477-2015, 2015.
 1205

1206 Twomey, S., The influence of pollution on the shortwave albedo of clouds, *J. Atmos. Sci.*, 34, 1149 – 1152,
 1207 DOI: [http://dx.doi.org/10.1175/1520-0469\(1977\)034](http://dx.doi.org/10.1175/1520-0469(1977)034), 1977.
 1208

1209 Wang, K. C., R. E. Dickinson, and S. L. Liang, Clear-sky visibility has decrease over land globally from 1973 to
 1210 2007, *Science*, 323, 1468–1470, doi:10.1126/science.1167549, 2009.
 1211

1212 Wild, M., Global dimming and brightening: A review, *J. Geophys. Res.*, 114, D00D16,
 1213 doi:10.1029/2008JD011470, 2009.
 1214

1215 Wild, M., H. Gilgen, A. Roesch, A. Ohmura, C. N. Long, E. G. Dutton, B. Forgan, A. Kallis, V. Russak, A.
 1216 Tsvetkov, From Dimming to Brightening: Decadal Changes in Solar Radiation at Earth's surface. *Science*, 308,
 1217 , 847, Doi: 10.1126/science.1103215, 2005.
 1218

1219 Wild, M., Introduction to special section on Global Dimming and Brightening, *J. Geophys. Res.*, 115, D00D00,
 1220 doi:10.1029/2009JD012841, 2010.

1221

1222 World Meteorological Organization (WMO), WMO guide to meteorological instruments and methods of
1223 observation, 7th ed., WMO-No. 8, Geneva, Switzerland, 2008.

1224

1225 Wu, J., J. Luo, L. Zhang, L. Xia, D. Zhao, and J. Tang, Improvement of aerosol optical depth retrieval using
1226 visibility data in China during the past 50 years, *J. Geophys. Res.*, 119, 13,370–13,387,
1227 doi:10.1002/2014JD021550, 2014.

1228